Partitioning gross primary production of a boreal forest among species and strata: A multi-method approach☆

Antoine Vernay [a,b,*], Niles Hasselquist [a], Kersti Leppä [c], Anne Klosterhalfen [a,d], Jose Gutierrez Lopez [a], Zsofia R Stangl [a], Jinshu Chi [a,h], Nathaliia Kozii [a], John D Marshall [a,e,f,g]

[a] Department of Forest Ecology and Management, Swedish University of Agricultural Sciences, 901 83 Umeå, Sweden
[b] Univ Lyon, Université Claude Bernard Lyon 1, CNRS, ENTPE, UMR 5023 LEHNA F-69622 Villeurbanne, France
[c] Natural Resources Institute Finland (Luke), FI-00790 Helsinki, Finland
[d] Bioclimatology, University of Göttingen, 37077 Göttingen, Germany
[e] Leibniz-Zentrum für Agrarlandschaftsforschung, 15374 Müncheberg, Germany
[f] Department of Geological Sciences, Gothenburg University, Gothenburg, Sweden
[g] Department of Energy and Matter Fluxes, Czech Globe, Belidla, Czechia
[h] Earth, Ocean and Atmospheric Sciences Thrust, The Hong Kong University of Science and Technology (Guangzhou), 511453 Guangzhou, China

ARTICLE INFO

ABSTRACT

We compared three methods of estimating gross primary production (GPP) of a boreal forest dominated by spruce and pine with the goals of 1) converging on the best estimate and 2) disaggregating the GPP among the two canopy species and the understory stratum. The three methods were: 1) eddy covariance (EC), 2) a soil-vegetation-atmosphere transfer model, APES, driven by meteorological data, and 3) an ecophysiological approach (Iso/SF) based on sap flux and phloem δ^{13}C, where sap flux is used to estimate stomatal conductance and δ^{13}C is used to estimate intrinsic water-use efficiency (WUE_i). The EC and APES methods agreed rather well, which was expected because APES was developed to predict eddy covariance data. The Iso/SF method, which is based on independent data, yielded lower estimates. This was partly because it excluded understory vegetation from the GPP estimate. We also found that the measured sap flux/transpiration estimates for spruce in Iso/SF were much lower than those from APES. In contrast, the absolute values for Scots pines were very similar between the two methods, especially in the summer. In both species, the seasonal dynamics match well among all methods. This multi-method approach allowed us to detect possible problems in the spruce sap-flux measurements, but successfully upscaled pine data from ecophysiological traits to stand and ecosystem functioning.

1. Introduction

Approaches for estimating ecosystem GPP can be broadly categorized into top-down or bottom-up. The bottom-up estimates rely on ecophysiological or gas exchange data at individual or mesocosm level, which are then scaled up to ecosystem-level (Kim et al., 2008; Klein et al., 2016; Peichl et al., 2010; Vernay et al., 2020). Top-down approaches derive GPP from ecosystem-scale measurements, for instance based on the eddy covariance (EC) method (Baldocchi, 2020; Ouimette et al., 2018).

Each approach has advantages and disadvantages. At the ecosystem scale, net CO_2 ecosystem exchange (NEE) and evapotranspiration (as latent heat flux) are commonly estimated with EC flux towers providing continuous data at a high temporal resolution without disturbing ecosystem and experimental conditions. Currently, EC data are obtained with about 1400 flux towers within various ecosystem types around the world (Baldocchi, 2014, 2003; Burba, 2019; Falge et al., 2017). Most flux sites are part of vast networks (e.g., FLUXNET,[1] ICOS[2]) and submit their data to databases following standardized protocols and methods for data processing. Due to the constant improvement of data processing

strategies (quality-check and acquisition, flux estimation, etc.), the EC method is considered robust, at least by the eddy covariance community. However, not all limitations in EC flux estimates can be prevented, such as the need to be set on flat terrain (Hollinger and Richardson, 2005; Jung et al., 2020). Some uncertainties in flux estimates are introduced for time periods with stable atmospheric conditions, where, especially in dense forest canopies, the requirement for sufficient turbulent exchange between the ecosystem and the atmosphere above may not be met. Thus, one basic assumption of the EC method would be violated. However, these periods of low turbulence can be filtered out (e. g., Jocher et al., 2017; Thomas et al., 2013; Wutzler et al., 2018). Finally, the obtained NEE can be partitioned into its component fluxes, GPP and ecosystem respiration (R_{eco}), using various models (Baldocchi, 2003; Lasslop et al., 2010; Loescher et al., 2006; Luyssaert et al., 2007; Reichstein et al., 2012, 2005). Multiple studies have compared these source partitioning methods and discussed their advantages and disadvantages (e.g., Chi et al., 2021; Klosterhalfen et al., 2019; Marshall et al., 2023; Stoy et al., 2006).

GPP can also be estimated using semi-empirical models (Minunno et al., 2016; Tian et al., 2020) or mechanistic multi-layer soil-vegetation-atmosphere transfer models, such as the APES model (Baldocchi et al., 2002; Launiainen et al., 2015; Ogée et al., 2003). Indeed, mechanistic soil-vegetation-atmosphere transfer models, which are based on leaf-level energy balance and gas exchange, are less reliant on site-specific calibration than more empirical models, making them a highly attractive tool to estimate GPP. Although these method/models provide a degree of independence from EC data, in fact they are usually calibrated using EC data. Consequently, any bias in the EC method (including meteorological data), may be carried forward into the model structure and its fitted parameters. Nonetheless, the APES model is attractive because it can partition C fluxes between understory vs overstory strata and also among tree species in the overstory, making it particularly well suited for comparison to ecophysiological data measures at individual/mesocosm scale.

Finally, ecophysiological approaches, such as gas exchange chambers and sap flow, require a different set of measurements and assumptions and thus are more independent of EC-based methods. In particular, the estimation of tree transpiration from sap-flow measurements and phloem isotopic $\delta^{13}C$ (Iso/SF) has recently been used to estimate GPP at a stand scale (Hu et al., 2010; Klein et al., 2016; Vernay et al., 2020). This method infers GPP from tree transpiration (Q) and tree intrinsic water use efficiency (WUE_i). Basically, it may be summarized as GPP = $Q \times WUE_i$. If these variables are estimated from a representative sample collection then it can infer GPP at stand scale.(Grime, 1998) Three potential challenges of the Iso/SF method are the requirement for a mesophyll conductance correction, which is frequently difficult to obtain due to the complex experimental setup (Stangl et al., 2019), the need to measure $\delta^{13}C$ so that it reflects seasonal variation and integrates over the tree canopy, and finally, the requirement for quantitative estimates of sap flow. The sap-flow data, particularly when heat dissipation methods are used (Oren et al., 1999), is further hampered by the difficulty of estimating stomatal conductance at low vapour pressure deficits, which are common in the early and late photosynthetic season. However, this is commonly addressed with the use of alternative heat-pulse methods that are very sensitive to small flows (Burgess et al. 2001, Gutierrez Lopez et al. 2021). Additionally, issues remain regarding the description of radial distributions across the conductive tissue of the tree (Berdanier et al., 2016; Caylor and Dragoni, 2009; Granier et al., 1994; Wullschleger and King, 2000).

GPP estimates obtained by different methods can be compared for their seasonal trends, day-to-day dynamics, and for their daily and annual absolute values. Most methods are able to describe the same bell-shaped seasonal pattern of GPP, typical for boreal forests. Indeed, studies at global scales showed that the dynamics of GPP difference were rather similar between methods (Campioli et al., 2016; Wang et al., 2017). However, the absolute values may strongly differ. Comparisons

between EC and chamber approaches (Peichl et al., 2010) or EC-based method and isotopic/sap-flow methods (Vernay et al., 2020) have confirmed differences among methods; generally, chambers and Iso/SF methods have produced higher GPP estimates than EC-based data (Peichl et al., 2010; Vernay et al., 2020; Wang et al., 2010).

In addition to GPP estimates at ecosystem scale, different methods have different capabilities to estimate the partitioning of GPP into different species and into different forest strata. Consequently, the source partitioning is of great interest because different sections of the forest, such as the understory, can be very important in the C flux of boreal forests (Ikawa et al., 2015; Palmroth et al., 2019). Partitioning GPP brings more information ecosystem functioning, complementary to GPP at ecosystem scale estimates presented before. Several studies have partitioned GPP data among different strata and species within a stand (Chi et al., 2021; Misson et al., 2007; Palmroth et al., 2019). The partitioning to over- and understory has most often been done using semi-empirical models (Ikawa et al., 2015; Misson et al., 2007; Tian et al., 2021). Recently, source partitioning of C fluxes of over- and understory has been conducted with measurements of two separate EC systems, one above and one below the canopy (Chi et al., 2021). This empirical description of above- vs. below-canopy, provides an intermediate step toward disaggregation among species. Soil-plant-atmosphere transfer models such as the APES model (Launiainen et al., 2015), which support the description of multiple species in the overstory canopy in addition to the understory vegetation, can be used to address the contribution of individual species to ecosystem fluxes. This makes such models particularly well suited for comparisons to multi-scale data. However, such models require trait parameterizations by species.

Given that all methods present advantages and disadvantages, a multi-methods approach would help to give a larger overview of the GPP variability and its underlying drivers (Schäfer et al., 2003), where estimates and their implications are not tied to the assumptions or disadvantages of a single method, but rather are further validated by multiple approaches. Consequently, a multi-methods comparison could help to disentangle the processes embedded in each method and help understand discrepancies between GPP estimates. In other words, the greatest advantage of a multi-method approach is its complementary nature.

In this study, we estimated GPP of a mixed boreal forest using three different methods: EC, a soil-vegetation-atmosphere transfer model (APES, Launiainen et al., 2015), and Iso/SF. Our objectives were twofold: first, to estimate GPP variability in a multi-method comparison and consider how the different method assumptions could explain the intra-method variability. Second, we estimated the species and strata contributions to the stand-scale GPP. We hypothesized that:

  (i) The different methods captured the same seasonal GPP dynamics with absolute values within the similar uncertainty range. Further, we hypothesized that the discrepancies between methods occurred primarily when environmental data showed high variability (spring and summer).

 (ii) APES and Iso/SF methods estimate similar species contributions to the total canopy GPP based on their abundance, phenology, and physiological characteristics.

(iii) Methods that estimate GPP at ecosystem scale (EC and APES) should have a higher GPP than method using only tree canopy GPP (Iso/SF).

2. Materials and methods

For this multi-method comparison, we applied the eddy-covariance, APES and Iso/SF methods on the same mixed boreal forest in the same year. The methods we tested, have been studied individually in various other ecosystems, but to our knowledge, this is the first time they are systematically compared in a typical pine-spruce mixed boreal ecosystem, which is known to have extreme weather variability during

the growing season. It influences all vegetation strata, which potentially limiting the predicting capabilities of methods. The materials and methods section describes first the site and stand features, which were common to all methods, and then the details of each method application and the applied correction to account for site features.

2.1. Study site

This study was conducted at Svartberget experimental forest, located within the Krycklan catchment area (www.slu.se/Krycklan) in northern Sweden (64°15′N, 19°46′E, 270 m a.s.l.), in 2019. The climate there is a cold temperate humid according to the Köppen classification (Kottek et al., 2006) with a mean annual temperature of 1.8°C and annual precipitation of 623 mm yr^{-1} (averaging period 1981–2010, Laudon et al., 2021).

Most of the catchment area is covered by a mixed forest of pine and spruce (87 %). Understory vegetation at the site is characterized by bilberry (*Vaccinium myrtillus*) and lingonberry (*Vaccinium vitis-idaea*) with mosses (*Pleurozium schreberi* and *Hylocomium splendens*) in the bottom layer (Laudon et al., 2013). Soils have been formed in a quaternary till deposit and display a podzolic layer. Organic histosols are found in the riparian zone (Ledesma et al., 2016). The catchment was highly instrumented to characterize soil, hydrological, and meteorological properties. Moreover, since 2011, the Svartberget site belongs to
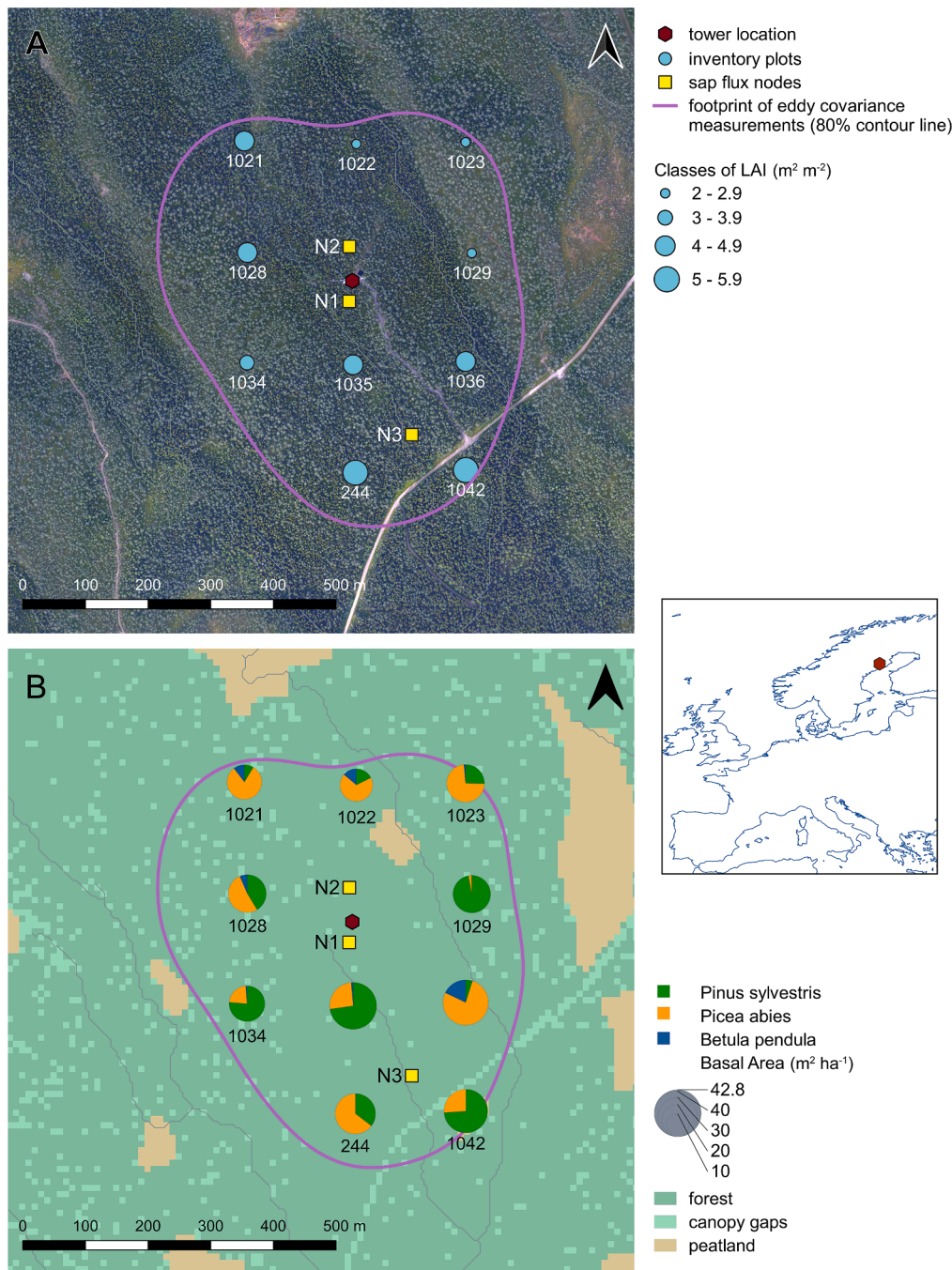
Fig. 1. Subcatchment of the Kyrcklan catchment where the study took place in Svartberget (red point on the Europe map). The orthophoto in panel (A) and environmental data of inventory plots in both panels were obtained by the Swedish University of Agricultural Sciences and Swedish Forest Agency in Umea and the geospatial data of the land cover types in panel (B) were taken from Chi et al. (2019) (Geografiska™ Sverigedata product).

the Integrated Carbon Observation System (ICOS) network with a 150 m flux tower. The tower has been equipped with eddy covariance sensors to measure gas exchanges (more information can be found on the website: https://sweden.icos-cp.eu/Svartberget). The tower is located on a mild slope (less than 4 %) facing South-East. The height differences within the footprint and in the main wind direction (between North-West and North) is about 45 m.

2.2. Stand characteristics

Stand characteristics (species abundance, diameter at breast height) were available from regularly spaced forest 10-m inventory plots (Fig. 1) in the approximately 70 km² Krycklan catchment. We selected the ten inventory plots inside subcatchment C2, within which the EC tower is centrally located. On average, stand basal area was 30 m² ha⁻¹ and the shares of Scots pine (*Pinus sylvestris*, PS), Norway spruce (*Picea abies*, PA), and birch (*Betula pendula*, BP) were 46%, 49 %, and 5 %, respectively. In June-July 2018, projected leaf area index (LAI) was measured in the stands with the LAI-2200C Plant Canopy Analyzer (Selin, 2020). LAI varied from 2.5 to 5.1 m² m^{-2} for the whole plots. LAI of pine was on average (from ten plots) 1.23 m² m^{-2} ($\pm$1.0 m² m^{-2}) while that of spruce was 2.53 m² m^{-2} ($\pm$1.2 m² m^{-2}).

2.3. Environmental data

The ICOS Svartberget ecosystem–atmosphere station provided data on greenhouse gas, water vapour, and energy fluxes as well as meteorological, vegetation, and soil environmental variables (http://www.icos-sweden.se/station_svartberget.html). Environmental data, air temperature (T_a, °C), relative humidity (RH,%), air pressure (P_{atm}, kPa), photosynthetic photon flux density (PPFD, µmol $m^{-2} s^{-1}$), precipitation (mm), soil water content (SWC,%), atmospheric CO_2 concentration (C_a, ppm), soil temperature (T_{soil}, °C), wind speed (m s^{-1}) and incoming shortwave and longwave radiation were available as half-hourly averages. Daily averages are presented in Fig. 2.

From RH and T_a, we inferred the vapour pressure deficit during daytime (VPD$_d$, kPa), i.e., when PPFD was >30 µmol $m^{-2} s^{-1}$, as follows (Ngao et al., 2017):

$$VPD_d = \left(0.6108 \times e^{\frac{17.27 \times T_d}{T_a + 237.3}}\right) \times \left(1 - \frac{RH}{100}\right) \quad (1)$$

Then, we calculated the daylength normalized VPD (D$_Z$, kPa) (Oren et al., 1996) as follows:

$$D_Z = VPD_d \times \left(\frac{n_d}{24}\right) \quad (2)$$

with n$_d$ the number of daylight hours ($\geq$30 µmol PPFD $m^{-2} s^{-1}$) (24 represents the 24 h of one day). These daily D$_Z$ were summed and used to reduce the influence of diurnal variation (Oren et al., 1996) and allow us to focus on the seasonal patterns. Dz combines the daytime VPD$_d$ with daylength into a synthetic variable, which is commonly applied in the sap-flux literature. To be consistent with that literature, we have also used this variable.

In all methods used to estimate GPP at stand scale (EC, APES, Iso/SF), we only considered daytime values (i.e. when PPFD was $\geq$30 µmol $m^{-2} s^{-1}$). We assumed that there was no photosynthesis during nighttime (but see, Kooijmans et al., 2017).

To provide context for the GPP estimate, we defined the thermal growing season as the period beginning after the occurrence of five consecutive days with mean daily temperature > 5 °C and the end was defined as the occurrence of five consecutive days <5 °C (Cornes et al., 2019; Mäkelä et al., 2006). In 2019, the thermal growing season lasted from April 15 (DOY 105) to September 17 (DOY 260), which represented 156 days (Fig. 2). Note that GPP was calculated for the entire year, not only during the growing season.

2.4. Isotopic/sap-flux method

2.4.1. GPP estimate from isotopic and sap-flux data

With the Iso/SF method GPP for individual trees was inferred and then scaled up to the stand level (GPP$_{Iso/SF}$, g C $m^{-2} d^{-1}$). Broadly, GPP$_{Iso/SF}$ was obtained by multiplying the intrinsic water-use efficiency (WUE$_i$) by canopy stomatal conductance (g$_s$), where WUE$_i$ was estimated from phloem δ^{13}C and g$_s$ was estimated from tree-stem sap flux and daylength normalized mean vapour pressure deficit (D$_Z$). Because birches represented a negligible basal area compared to spruce and pines at the study site, we did not consider this species in the Iso/SF calculation.

2.4.2. Sap-flux and transpiration measurements to estimate canopy stomatal conductance

Within the studied area (Fig. 1), we selected three locations (hereafter: nodes) to measure tree-level transpiration (Q, L day⁻¹). Each node was located along a topographic gradient: Footslope (low), backslope (middle), and shoulder slope (high) within an elevation range of 260–285 m a.s.l. Within each node (25 m radius), we selected 20 trees
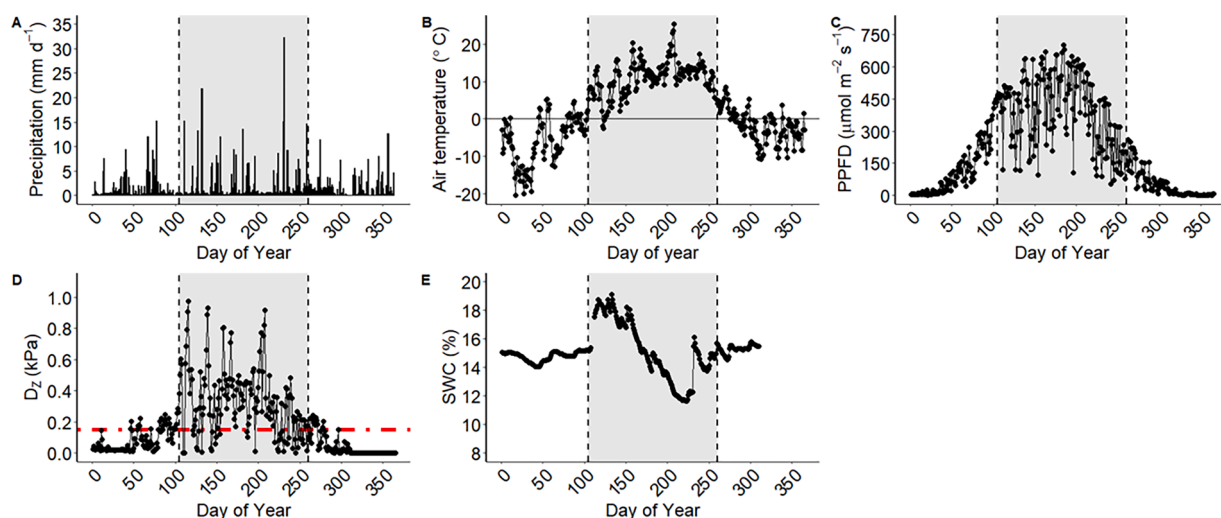

Fig. 2. Environmental data at Svartberget site in 2019, (A) daily precipitation sum, (B) daily mean air temperature, (C) daily mean photosynthetic photon flux density (PPFD), (D) daily normalized vapour pressure deficit (Dz) during daylight hours, where the red dashed line was the minimal threshold, 0.15 kPa, considered in GPPIso/SF calculations, (E) daily mean volumetric soil water content at 10 cm (%, SWC). Grey area represents the thermal growing season.

(10 pine and 10 spruce) that represented the diameter distribution of trees in the entire studied area. Sap-flux density (JS, $cm^3\,cm^{-2}\,h^{-1}$) was measured at breast height using custom-made heat dissipation-type sap-flow sensors (Granier, 1987, 1985; Gutiérrez López, 2015). These sensors were installed in 2016 on selected trees and all sensors were covered with reflective insulation to minimize the effect of natural temperature gradients. To account for radial and circumferential variability in JS (Berdanier et al., 2016; Caylor and Dragoni, 2009; Granier et al., 1994; Wullschleger and King, 2000), we installed sensors at four sapwood depths (i.e., 0–20 mm, 20–40 mm, 40–60 mm, and 60–80 mm) in a subset of trees (five per species per node). Additionally, we installed sensors in the four cardinal directions on the stems of six selected trees ($n = 3$ per species). In total, we installed 150 sap-flow sensors on 60 trees (20 trees per node). Differential voltage (DiffV, mV) between the heated and the reference probe was read every 30 s and stored as 30-minute averages using one data logger (CR1000X, Campbell Scientific) per node.

Due to the long-term nature of our sap-flow data, we corrected for wounding drift (the cumulative changes in sensor sensibility over time due to the formation of scar tissue; Flo et al., 2019; Kitin et al., 2010; McElrone et al., 2010; Peters et al., 2018), deploying eight additional heat dissipation (HD) sensors in spring of 2019 on eight trees ($n = 4$ per species) that already had HD sensors from the beginning of this study, and estimated a percent reduction in JS over time by species. Further information about correction and details of data processing and upscaling to canopy scale are provided in Gutierrez Lopez et al. (2021).

Canopy conductance for water vapour (g_S, mol $H_2O\,m^{-2}d^{-1}$) was estimated for each tree species at stand scale as follows:

$$g_S = \frac{(Q/M_{H2O})}{\frac{VPD_d}{P_{atm}}} \times 1000 \tag{3}$$

Q is the species sum of transpiration at stand scale (mm d^{-1}), M_{H2O} the molar mass of water (18 g mol^{-1}), and P_{atm} the atmospheric pressure (kPa).

Two corrections were applied to g_S to account for boreal conditions: firstly, VPD (and D_Z) could be very low and thus strongly influenced g_S ($\lim_{VPD_z \to 0} g_S \infty$) when it tended to 0 (Fig. 2, Eq. (3)). To remove a part of this noise and constrain the maximum value of gs, we chose to replace D_Z values below 0.15 kPa with 0.15 kPa. Secondly, g_S was corrected for the acclimation of photosynthetic capacity outside the thermal growing season, when sap flux may be very low and less correlated to photosynthetic activity. We justify g_S correction because natural selection is expected to disfavour stomatal opening when photosynthesis is impossible (Mäkelä et al., 2004). Further, it is recognized that water flow occurs as stems freeze and thaw even before photosynthesis has begun. We were eager to avoid the inference of stomatal conductance from these internal redistributions (Charrier et al., 2017). We used a temperature-based function proposed by Mäkelä et al. (2008) for Scots pines to estimate daily and maximal photosynthetic capacity ($Â$ and $Â_{max}$) in 2019. Then, g_S became $g_{SÂ}$:

$$g_{SÂ} = min\left\{\frac{Â}{Â_{max}}, 1\right\} \times g_S \tag{4}$$

We then applied $g_{SÂ}$ to DOY (day of year) between 260 and 105 as follows:

$$GPP_{Iso/SF} = \begin{cases} if\ DOY\langle105\ or\ DOY\rangle260,\ WUE_i \times g_{SÂ} \times \frac{M_C}{10^6} \\ if\ 105 < DOY < 260,\ WUE_i \times g_S \times \frac{M_C}{10^6} \end{cases} \tag{5}$$

with M_C the molar mass of C (12 g mol^{-1}), WUE_i the intrinsic water use efficiency (µmol CO_2 mol H_2O^{-1}) and g_S and $g_{SÂ}$, the non-corrected and corrected canopy stomatal conductance (mol $H_2O\,m^{-2}\,d^{-1}$), respectively. Dates were chosen based on low values for the temperature function.

2.4.3. Phloem sampling and $\delta^{13}C$ measurements

The phloem sampling was carried out within the three sap-flux measurement nodes (Fig. 1). In each node, we selected four trees per species to represent the largest range of tree height and diameter of the sub-catchment. The dataset was balanced with 12 trees per species, covering the diameter gradient in the stand. This led to a total of 4 replicates × 2 tree species × 3 complete nodes, $n = 24$ trees sampled per sampling date. Phloem samples were collected every four weeks from 2 May 2019 to 16 October 2019.

To measure the $\delta^{13}C$ of the solutes in the phloem sap ($\delta^{13}C_p$, ‰), we sampled phloem discs at breast height on the trunk using a cork-borer 9 mm in diameter (Gerle et al., 2023). In the field, we carefully removed bark and wood to isolate the active phloem. This phloem disc was immersed into a 6 mL vial containing 2 mL of de-ionised water for exudation. The exudation lasted for five hours (Gessler et al., 2004), after which the exudate solution was stored in a freezer until it was freeze-dried. The solutes were redissolved in 150 µL de-ionised water and the resulting solution was pipetted into tin capsules and dried at 60 °C for 12 h. The samples were then loaded into an elemental analyser (NA 2500; CE Instruments, Milan, Italy) coupled to an isotope ratio mass spectrometer (Delta Plus; Finnigan MAT GmbH, Bremen, Germany) for $\delta^{13}C$ analysis, performed at the SLU stable isotope laboratory (SSIL, Umeå, Sweden, www.slu.se/en/departments/forest-ecology-management/ssil). Isotopic results were expressed in ‰ relative to VPDB (Vienna Pee Dee Belemnite).

In order to estimate the isotopic discrimination against ^{13}C ($\Delta^{13}C$, ‰), we combined atmospheric and phloem $\delta^{13}C$ values. We used the atmospheric $\delta^{13}C$ ($\delta^{13}C_a$, ‰) provided by the National Oceanic and Atmospheric Administration database using the nearest sample station, at Pallas-Sammaltunturi in Finland (White et al., 2015). This was necessary to account for the large seasonal cycle of $\delta^{13}C_a$ at high latitudes.

Then, Δ was calculated as follows:

$$\Delta = \frac{\delta^{13}C_a - \delta^{13}C_p}{1 + \left(\frac{\delta^{13}C_p}{1000}\right)} \tag{6}$$

There is debate about whether $\delta^{13}C_p$ correctly represents fresh photosynthates (e.g., Offermann et al., 2011). We acknowledge that post-photosynthetic pathways might alter the $\delta^{13}C_p$, but our previous work suggests that these effects are negligible, at least in pine (Vernay et al., 2020).

2.4.4. Mesophyll conductance estimation

Gas-exchange and ^{13}C discrimination of upper-canopy shoots of mature *Pinus sylvestris* were measured continuously for the entire growing season of 2017, and the data were used to estimate the ratio of stomatal conductance (g_S) to mesophyll conductance g_m (g_S/g_m). The measurement system was described in detail by Stangl et al. (2019). Gas-exchange parameters were estimated according to Farquhar et al. (1980), and g_m was estimated according to the model proposed by Busch et al. (2020). The seasonal median of g_S/g_m was 0.60, representing an integrating value of the ratio along the growing season (Stangl et al., 2022). The ratio was assumed constant in our subsequent calculations. This choice made the Iso/SF method as simple as possible and yet allowed for the seasonal variability of g_m.

The g_S/g_m ratio of *Picea abies* was estimated from ^{13}C discrimination measurements on upper canopy leaves in August 2019. An Li-6400Xt portable photosynthesis system (Licor Biosciences Ltd.) was coupled to a cavity ring-down spectrophotometer (G2131-i, Picarro Inc., California, USA) for the simultaneous measurement of gas-exchange and ^{13}C

discrimination. The ratio of conductances was estimated the same way as for *P. sylvestris*. The mean g_S/g_m was 0.68 ± 0.1 for *P. abies*. As with pine, this ratio was considered constant over the growing season.

2.4.5. Intrinsic water use efficiency calculation

We calculated the intrinsic water use efficiency (WUE$_i$, μmol CO_2 mol H_2O^{-1}) for each tree and calculated the mean per species according to (Seibt et al., 2008) for each phloem sampling day:

$$\text{WUE}_i = \frac{C_a}{r} \times \left[\frac{b - \Delta - f \times \left(\frac{\Gamma^*}{C_a} \right)}{b - a_a + (b - a_i) \times \frac{g_s}{g_m}} \right] \quad (7)$$

where C_a is the atmospheric CO_2 concentration (μmol^{-1}), r the ratio of diffusivities of water vapour relative to CO_2 in the air (1.6), b the fractionation during carboxylation (29 ‰), f the fractionation during photorespiration (16.2 ‰, Evans and Caemmerer, 2013), a_a and a_i the fractionation of the diffusion through the air (4.4 ‰) and the fractionation of diffusion and dissolution in water (1.8 ‰), respectively, and g_s/g_m is the ratio of stomatal to mesophyll conductance. The CO_2 compensation point (Γ^*, μmol mol^{-1}), was calculated according to the following formula (Medlyn et al., 2002):

$$\Gamma^* = 42.75, \times e^{\frac{3,783.0 \ \times .(T_K,-29,8)}{,298,\times T_K,\times R}} \quad (8)$$

with T_K the ambient temperature (K) and R the universal gas constant (8.314 J mol^{-1} K^{-1}).

We showed in a previous study that daytime respiration would have a negligible effect on WUE$_i$. Therefore we neglected this parameter to avoid introducing additional uncertainty (Vernay et al., 2020). We assumed that the mean WUE$_i$ per species represented the WUE$_i$ of the stand, as we sampled trees in the whole range of diameter. We then inferred the daily pattern of WUE$_i$, for the whole growing season, from the four-weekly measurements $\delta^{13}C_p$ and $\delta^{13}C_a$. Daily $\delta^{13}C_a$ and $\delta^{13}C_p$ data were modelled with the loess method (Cleveland et al., 1992) to estimate a daily value of Δ, as described in a previous study (Schiestl-Aalto et al., 2021).

2.5. Eddy covariance measurements

In the framework of the ICOS network, EC measurements have been conducted continuously at the Svartberget study site since 2014. The ICOS ecosystem-level EC system was mounted at 34.5 m in 2019 measuring CO_2, water vapour, and energy exchange between the boreal forest and the atmosphere. A below-canopy EC system was installed 2.5 m above the ground to measure the net CO_2 fluxes over the forest floor within the footprint of the above-canopy EC system. Thus, the 2-level set-up provided the opportunity to partition the CO_2 exchange between the under- and overstory (Chi et al., 2021). Furthermore, the EC measurements were quality-checked and filtered to remove periods with weak turbulent mixing, where the below-canopy air column was decoupled from the atmosphere above (Jocher et al., 2017). The measured above-canopy 30-min CO_2 flux was gap-filled and partitioned into the two flux components, GPP and R_{eco}, on stand scale using the R-package REddyProc (v3.6.3, Wutzler et al., 2018). Here, we investigated the GPP derived with the nighttime (GPP$_{EC\_NT}$) and daytime (GPP$_{EC\_DT}$) flux-based partitioning methods after Reichstein et al. (2005) and Lasslop et al. (2010), respectively. Further information about data processing, corrections, quality checks and controls, and final estimations of GPP can be found in Chi et al. (2019), Jocher et al. (2017), Montagnani et al. (2018), Sabbatini et al. (2018), and Thomas et al. (2013). Half-hourly GPP was then aggregated into daily sums. Furthermore, daytime GPP was aggregated from the half-hourly data only considering time steps with PPFD > 30 μmol m^{-2} s^{-1}.

We estimated flux footprints using the two-dimensional parameterization after Kljun et al. (2015). The method was applied to the quality-checked, half-hourly turbulence data. Furthermore, the footprint climatology was derived only for time steps with PPFD > 30 μmol m^{-2} s^{-1} during the thermal growing season, when the canopy was presumably photosynthetically active. Finally, the tree inventory plots within the area of the 80 % footprint flux fraction were selected (Fig. 1). That area contained the 3 nodes used in the Iso/SF approach and ten of the plots used for the APES simulations (cf. Sections 2.4 and 2.6).

2.6. APES model

APES describes the forest ecosystem as a one-dimensional column consisting of a multi-layer multi-species tree stand, a vegetation layer under the tree canopy, a forest floor covered by mosses or litter, and an underlying soil profile (Launiainen et al., 2015). As forcing variables, the model uses time-averaged (here half-hourly) meteorological variables at a reference level above the canopy. Forcing variables are precipitation, downwelling longwave radiation, direct and diffuse photosynthetically active and near-infrared radiation, wind speed, atmospheric pressure, air temperature, and mixing ratios of H_2O and CO_2. Additionally, here we used measured soil moisture and soil temperature at the depth of 0.05 m as lower boundary conditions for the model.

Canopy structure is conceptualized in the model as a layered horizontally homogeneous porous medium characterized by a leaf area density (LAD, m^2 leaves m^{-3}) distribution. LAD allocates LAI among canopy heights. Within the canopy, the model solves the transfer and absorption of shortwave and longwave radiation (Zhao et al., 2005; Zhao and Qualls, 2006), and the turbulent transport of scalars (air temperature, H2O, CO2) and momentum. The turbulent transport in the canopy air space and resulting vertical gradients of wind speed, air temperature, H_2O, and CO_2 are computed using standard first-order closure schemes (Launiainen et al., 2015). Partitioning of precipitation between interception and throughfall, as well as the energy balance of wet leaves, are solved in the canopy layers following Watanabe & Mizutani (1996).

Each plant type is characterized by its unique structural and physiological properties, including photosynthetic parameters, water use traits, and phenology. The coupled leaf gas and energy exchange is solved separately for sunlit (receiving diffuse and direct radiations) and shaded (receiving only diffuse radiations) leaves of each plant type and canopy layer using well-established solutions of coupled photosynthesis–stomatal conductance and leaf energy balance (Farquhar et al., 1980; Medlyn et al., 2011). During times without snow on the ground, the moss/litter layer is solved for water and energy balance and CO_2 exchange (Launiainen et al., 2015). Snow accumulation and melt is described here with a simple temperature-based approach and parameterized as in Launiainen et al. (2019).

The model was run for 10 stands with varying LAI and species contributions within the area of the 80 % footprint flux fraction of the EC measurements. For each stand, the share of LAI and LAD distributions of pine and spruce was estimated based on stand inventory data using allometric equations for needle/leaf biomass (Lehtonen et al., 2019; Tupek et al., 2015) and specific leaf area values (Härkönen et al., 2015). Normalized LAD distributions for each species were derived based on tree height following Tahvanainen & Forss (2008). The field layer vegetation was characterized by LAI = 0.6 m^2 m^{-2}. For a full list of model parameters, we refer the reader to Kozii et al. (2019), who applied the model to the same site. The average of the 10 model runs is used in the results.

2.7. Statistics

To compare the seasonal trends among the different methods, we used the loess function and 95 % confidence intervals over the season. Then, a pairwise comparison was done associated with a linear regression to estimate the intercept and slope of the regression. A pairwise

Spearman correlation was performed among methods and environmental data to search for explanations of mismatches among the methods. In the Iso/SF method we could test the effect of tree species and sampling date on WUE_i. We analyzed the difference between mean WUE_i values per species and sampling date with a linear mixed model (significance level $\alpha = 0.05$): tree species, sampling date and their interaction were tested. Tree identity (number and node) was used as a random factor. All data were tested to meet normality and homoscedasticity requirements and no transformation was necessary. To account for the repeated measurements, the regressions were run with a first-order autoregressive structure, applying the corAR1correlation option. To compare GPP among methods, we used a Deming regression to take into account the uncertainty of each method. The analyses were performed with the R nlme package (Pinheiro et al., 2016). The ANOVA function from 'car' library and multiple pairwise comparisons (library 'lsmeans' and 'multcompView') were performed. Graphs were drawn with help of ggplot package. Statistical analysis was performed under R Core Team (v4.0.3 2016) and Rstudio (2020).

3. Results

3.1. Environmental conditions

In 2019, the year of our comparison, total precipitation was 695 mm (Fig. 2A) and the mean air temperature was 2.5 °C (Fig. 2B). These values were both higher than the climatic averages (614 mm and 1.8 °C respectively, Laudon et al., 2021). PPFD started to increase in February and reached a maximum value at DOY 184 (701 μmol $m^{-2} s^{-1}$) before decreasing almost to zero in November (DOY 305, Fig. 2C). Dz was highly variable and showed the highest values during the thermal growing season. Dz rarely exceeded the 0.15 kPa threshold during winter but was generally above this limit during the thermal growing season (Fig. 2D). Finally, the SWC at 10 cm increased at the beginning of the thermal growing season, due to snow melt, but sharply dropped from DOY 133 to DOY 225 (Fig. 2E).

3.2. Daily transpiration and stomatal conductance per species at stand scale

Stand-scale transpiration derived from sap-flux measurements is an important component of the Iso/SF method. It is also estimated by the APES model. A comparison with evapotranspiration estimated with EC is proposed in Figs. A1 and A2 at stand scale. As shown in Fig. 3A, C and D, both methods depicted a strong seasonal pattern for each species. Norway spruces and Scots pines showed an increase of their transpiration rates at the beginning of the thermal growing season. The peak was reached at the end of July and then the transpiration rate decreased until mid-October, which is soon after the end of the thermal growing season. During the thermal growing season, the APES model showed higher values of transpiration rate than the Iso/SF method: transpiration rates based on Iso/SF method were 43 % and 58 % lower during the growing season than based on the APES model for Scots pines and Norway spruce, respectively (Fig. 3B and D. However, the day-to-day dynamics were similar between the two approaches ($R^2 = 0.83$ and 0.78 for Scots pines and Norway spruce respectively). Canopy conductance ($g_{SÂ}$) started to increase in March for both Scots pine and Norway spruce (Fig. A3). Norway spruce had the higher stand $g_{SÂ}$ values than the pines. Conductance decreased from August until the end of October for both species.
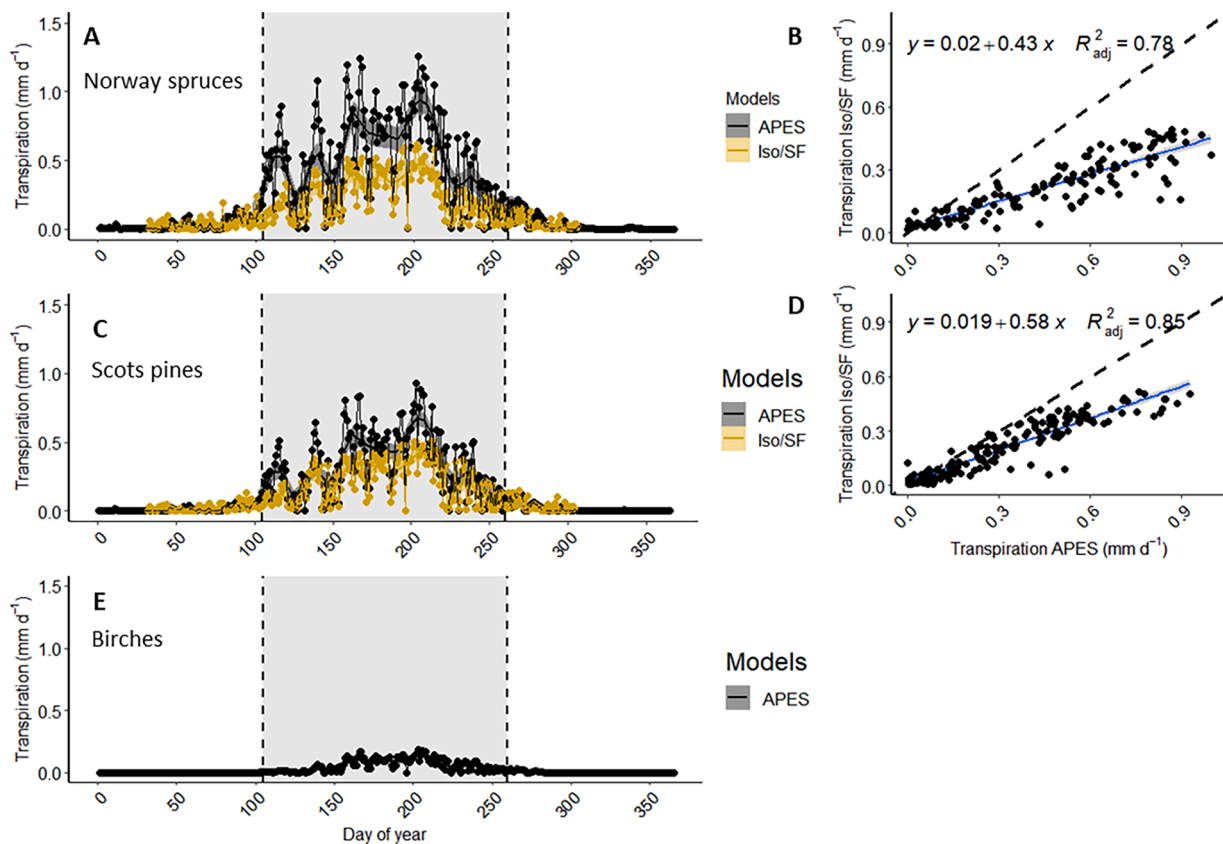
Fig. 3. Daily transpiration rate (mm d^{-1}, left panels) and APES vs Iso/SF methods comparisons during the growing season (right panels) for the main tree species in 2019, Norway spruce (*Picea abies*, panel A and B), Scots pine (*Pinus sylvestris*, panels C and D) and Birch (*Betula pendula*, panel E) estimated by APES model (black) or sap-flow measurements (gold). Dashed line represents the 1:1 relationship between the methods. Loess trend lines and 95 % confidence intervals were added. Grey area represents the thermal growing season.

3.3. WUE$_i$ per species

There was a significant effect of the date of sampling and tree species on the WUE$_i$ values (Fig. 4), but the interactions were not significant (DOY effect, $\chi^2 = 88$, df = 6, p-value<0.0001, tree species effect, $\chi^2 = 505$, df = 2, p-value<0.0001, and DOY × tree species effect $\chi^2 = 12$, df = 12, p-value= 0.42). The annual mean was significantly higher for Scots pine compared to Norway Spruce (annual mean WUE$_i$ ± SD for pines = 65 ± 7 µmol CO$_2$ mol H$_2$O^{-1}, spruces = 48 ± 10 µmol CO$_2$ mol H$_2$O^{-1}) (Fig. 4).

3.4. Daily and annual GPP comparison for the whole stand

The seasonal pattern of GPP was the same among the three methods (EC, APES and Iso/SF) (Fig. 5). We show here in the results GPP$_{EC\_DT}$ for the EC method instead of GPP$_{EC\_NT}$. Both GPP estimates based on the EC method were similar, as can be seen in Fig. A4D in the appendix, but GPP$_{EC\_DT}$ also considers the influence of VPD on daytime CO$_2$ assimilation, it is additionally based on daytime fluxes that are less impacted by decoupling events than nighttime fluxes, and it was closer to the other methods. Fig. A4A, B and C shows the influence of correction applied in the Iso/SF method.

In general, GPP was negligible until March, whereafter it started to increase. GPP began to increase before the beginning of the thermal growing season, but it increased more rapidly during the first part of the thermal growing season. The highest values were reached between mid-June (DOY 166) and mid-August (DOY 227) and then decreased rapidly until mid-October (DOY 288), which was about 25 days after the end of thermal growing season. By around DOY 315, GPP was essentially 0 g C $m^{-2} d^{-1}$.

APES and EC estimates were closely aligned except in mid-summer, when APES estimates were higher than EC estimates. This discrepancy coincides with high D$_Z$ and PPFD values, as shown in Fig. 2C and D. GPP$_{Iso/SF}$ estimates were lower than GPP$_{APES}$ or GPP$_{EC}$ estimates throughout the thermal growing season (Fig. 5), except during fall, when GPP$_{Iso/SF}$ became highly variable.

GPP estimates from each method are plotted against each other in the Fig. 6, according to the daily D$_Z$ and PPFD values. We chose to include these two drivers because they showed the highest correlations. The deviation from the 1:1 line was higher between GPP$_{Iso/SF}$ with GPP$_{APES}$ than between GPP$_{EC}$ with GPP$_{APES}$ and GPP$_{Iso/SF}$, which showed
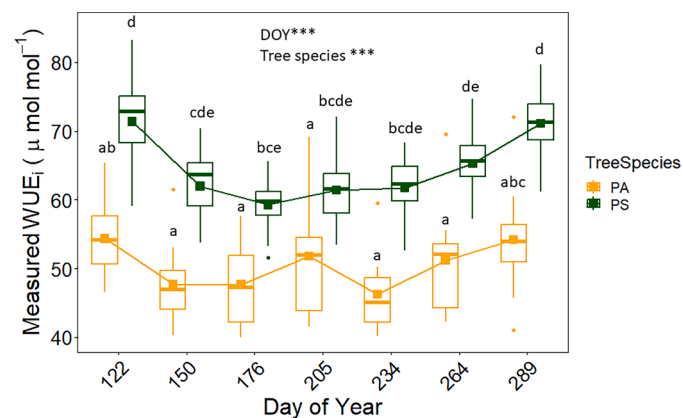
similar slopes. The intercept, however, was lower when GPP$_{Iso/SF}$ was plotted against GPP$_{APES}$ and GPP$_{EC}$, which confirmed a globally lower GPP$_{Iso/SF}$ estimate compared to other methods (Fig. 5). GPP$_{APES}$ and GPP$_{EC}$ had a very high coefficient of correlation (0.97). The correlations were lower for GPP$_{Iso/SF}$, but they still exceeded 0.8 (Fig. A5). The highest differences among GPP$_{Iso/SF}$, GPP$_{APES}$ and GPP$_{EC}$ occurred at the highest D$_Z$ values (Fig. 6). Similarly, the highest GPP differences between APES and EC seemed to occur for the highest D$_Z$ values (Fig. 5 and 6).

Annual sum of GPP showed different values between the EC and APES methods, but annual GPP estimated by the Iso/SF method was smaller (Fig. 7). Annual GPP$_{EC}$ was 917 gC m^{-2} (871 gC m^{-2} for over-story + 57 gC m^{-2} for understory). GPP$_{APES}$ was 1063 gC m^{-2} (966 gC m^{-2} for overstory + 97 gC m^{-2} for understory), but GPP$_{Iso/SF}$ was 697 gC m^{-2} for overstory only (Fig. 6). Focusing on overstory, the differences between the APES and EC methods, Iso/SF and EC methods, and APES and Iso/SF methods were 95, 174, and 269 gC m^{-2}, respectively.

3.5. Comparison of daily GPP between species

Focusing on species contributions, GPP$_{APES}$ and GPP$_{Iso/SF}$ were similar for their Scots pine estimates (360 and 350 gC m^{-2}, respectively), but quite different for Norway spruce (571 and 347 gC m^{-2}, respectively). GPP$_{Iso/SF}$ was, however, more variable from day to day than GPP$_{APES}$ for Scots pine during the fall 2019 (Fig. 8). Despite this variability, the low and high peaks compensated each other leading to a small annual sum difference (Fig. 7 and 8). Focusing on Norway spruce, GPP seasonal pattern between the APES and Iso/SF methods matched outside the thermal growing season but APES estimates were globally higher than Iso/SF estimates during the thermal growing season (Fig. 7 and 8).

3.6. Understory contribution to total GPP

Understory GPP$_{EC}$ and GPP$_{APES}$ increased from DOY 100 until DOY 201 and DOY 213, respectively (Fig. 9). Loess trends showed that APES values were globally higher than EC values during the thermal growing season. Understory GPP$_{EC}$ returned almost to 0 gC $m^{-2} d^{-1}$ after the end of the thermal growing season, around DOY 285. The annual sum of the understory GPP$_{EC}$ reached 57 gC m^{-2} for the whole year, i.e. 6 % of the annual sum estimated by EC, and GPP$_{APES}$ reached 97 gC m^{-2}, i.e. 11 % of the annual sum estimated by APES (Fig. 7).

4. Discussion

This study compared three methods using different approaches to estimate boreal forest GPP. It was not possible to determine which provides the "true" value, but we have highlighted concerns and strengths of each.

4.1. How well do the methods match? how can their different assumptions explain the potential mismatch?

The EC, APES and Iso/SF methods found similar seasonal trends for GPP. This result validates that any of these approaches may be used, with some caveats, to estimate GPP at stand scale. A similar study was performed recently, comparing Iso/SF methods and the PRELES model (semi-empirical model calibrated with EC data) in a monoculture forest and both methods agreed well as well (Vernay et al., 2020). The present study makes us confident for comparing qualitatively GPP estimates. Regarding the annual sum, EC and APES estimates gave similar results whereas Iso/SF showed a lower value, mainly due to the difference between APES and Iso/SF for *Picea abies* contribution. By drawing attention to this question, these results highlighted the benefit of a multimodel approach to underline the discrepancies. Indeed, all methods and models showed different daily values of GPP over the

Fig. 4. Intrinsic water use efficiency (WUE$_i$, µmol CO$_2$ mol H$_2$O^{-1}) derived from sampled phloem d^{13}C (Eq. (6)) for the two species, Norway spruce (*Picea abies* PA, yellow) and Scots pine (*Pinus sylvestris* PS, green). Squares show the mean value of WUE$_i$ (Eq. (7)) for the 4 trees per species sampled each day and the thick line within the boxplot represents the median value. Day of year (DOY) and the tree species factors had a significant effect on the WUE$_i$ variation (p-values<0.001). Letters show significant differences between tree species × sampling date factors after multiple Tukey test adjusted comparison between each tree species × sampling date.
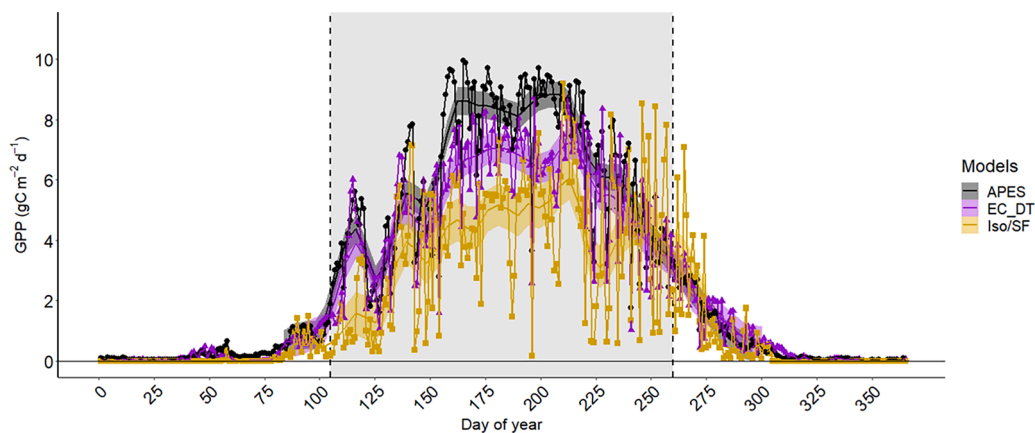
Fig. 5. Seasonal pattern of daytime GPP (g C m^{-2} d^{-1}) described by APES model (black), eddy covariance data (purple, after Lasslop et al. (2010) (EC_DT) and orange, after Reichstein et al. (2005) (EC_DT)), and Iso/SF method (gold) in 2019 at Svartberget site. 95 % confidence intervals were represented around loess trends of each approach. Grey area represents the thermal growing season.
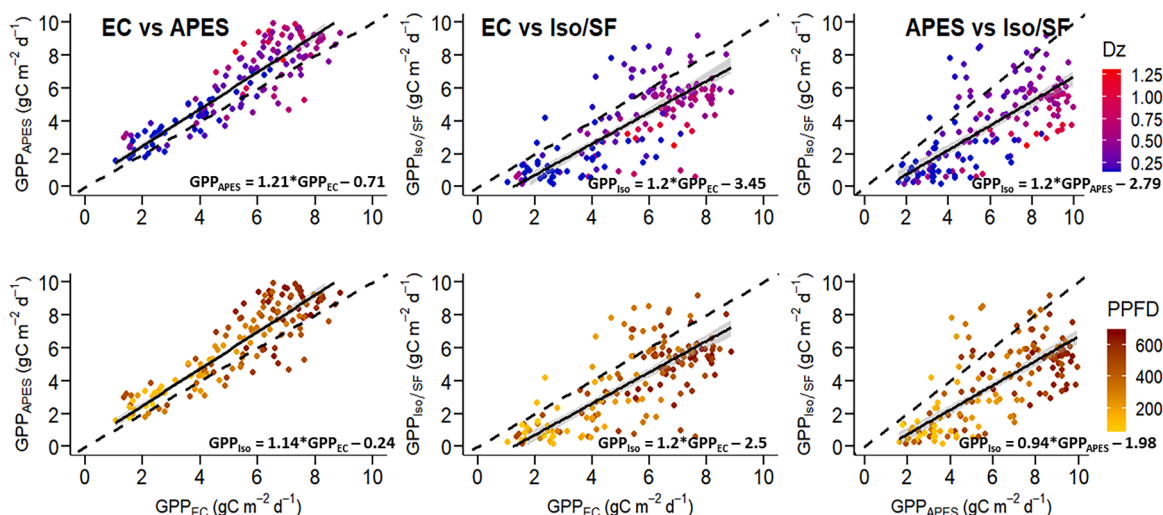

Fig. 6. Comparison of GPP estimates between EC_DT, APES, and Iso/SF approaches during the growing season. Each dot represents the cumulative daytime GPP of one day and the colour gradient the daily mean Dz (kPa, panels A, B and C) or daily mean PPFD (μmol m^{-2} s^{-1}, panels D, E and F), respectively. The dashed line represents the 1:1 relationship. The first column (panels A and D) compares GPP_{EC} vs GPP_{APES}, the second column (panels B and E) compares GPP_{EC} vs $GPP_{Iso/SF}$, and the third column compares GPP_{APES} vs $GPP_{Iso/SF}$. Equations of the Deming regression between methods were written on panels D, E and F for each model comparison.

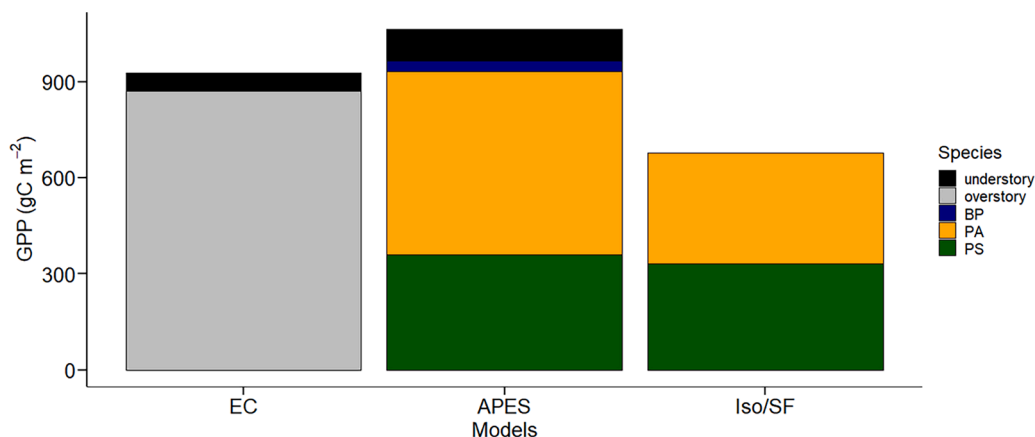**Fig. 7.** Annual sum of GPP (gC m^{-2}) for the three methods: eddy covariance (EC), APES and Iso/SF methods. The annual sum was disaggregated into the three main species present in the stand, Norway spruce (*Picea abies*, PA yellow), Scots pine (*Pinus sylvestris*, PS green), and Birch (*Betula pendula*, BP blue), as well as the understory. The EC method did not allow the partitioning into tree species (ecosystem GPP, grey) and Iso/SF did not account for the understory or Birch.
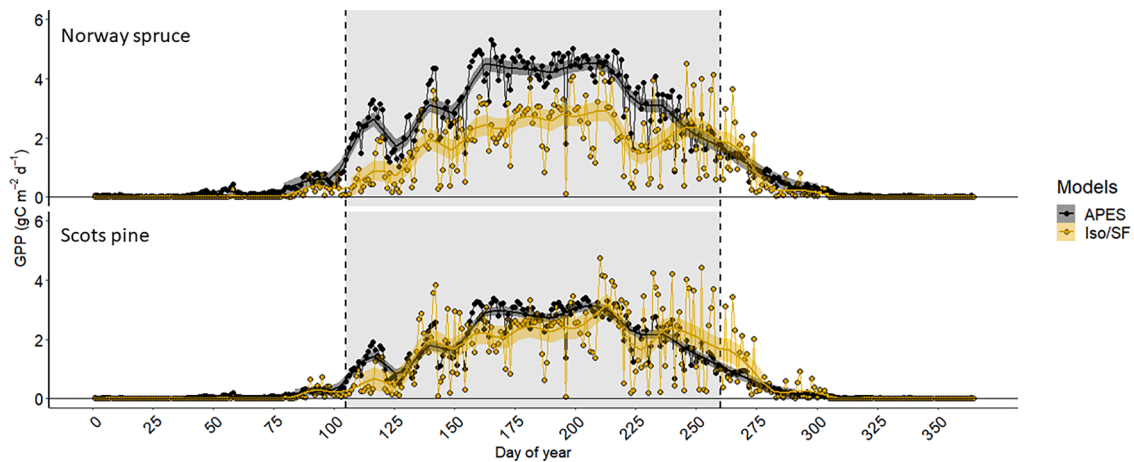
Fig. 8. Seasonal GPP pattern for the main tree species in 2019, Norway spruce (*Picea abies*, top panel) and Scots pine (*Pinus sylvestris*, bottom panel) estimated by APES model (black) or Iso/SF method (gold). Loess trend lines and 95 % confidence intervals were added. Grey area represents the thermal growing season.
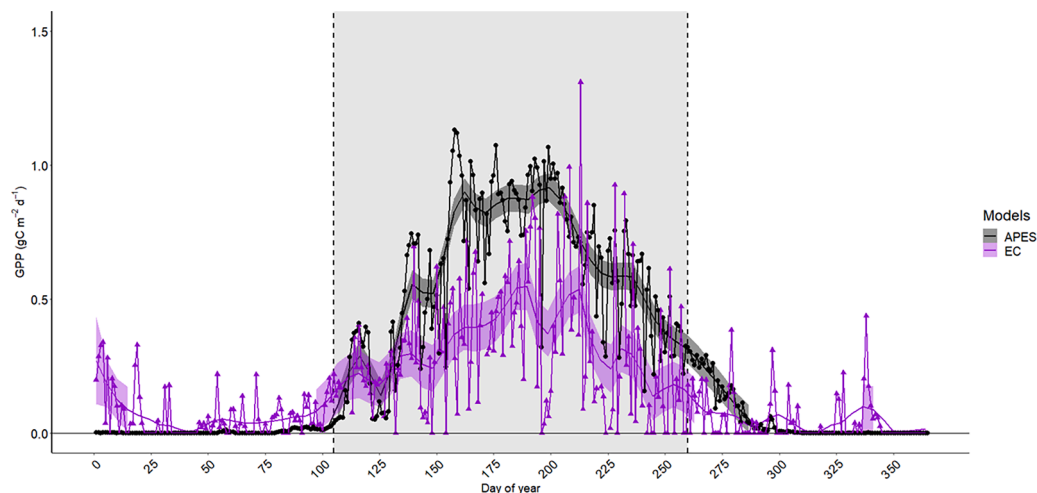

Fig. 9. Seasonal understory GPP_{EC} (purple) and GPP_{APES} (black) in 2019. Loess trend line and 95 % confidence intervals were added. Grey area represents the thermal growing season.

growing season leading to different annual sums. The absolute value of GPP, or selecting "the right method/model" requires that we first examine why they differ and which information about ecosystem they bring. In the following paragraphs, we try to decipher those discrepancies among method/models.

4.2. How can their different assumptions explain the potential mismatch?

The main criticism that might be applied to the EC data is the frequency of decoupling conditions in the early and late season (in this study, we considered the period before the start of the thermal growing season as the early season and the late season, at the end of the thermal growing season), which might modify fluxes due to advection of CO_2 to or from the site. Decoupling could limit the data availability during this critical time and might bias flux estimates, e.g., if the net advective flux were out of the footprint (Jocher et al., 2017). Indeed, the studied site was hilly and therefore, we filtered out decoupled periods and gap-filled them using the above-canopy EC systems. In total, additional 17 % of half-hourly NEE were filtered out due to decoupling (next to discarding half-hourly NEE due to other quality checks), where only a fourth of these decoupled periods occurred during daytime. Here, we mostly investigated daytime GPP and assumed fluxes to be zero during night-time, and we mostly considered fluxes aggregated to a daily time step, so that uncertainties due to quality checks and gap-filling were decreased.

However, there could be an additional decoupling near the ground surface (Thomas et al., 2013). These issues have largely not been emphasized because there has been no alternative test of the flux estimates, at least not for GPP. Thus, a comparison to other approaches, such as the Iso/SF method, becomes important.

Ecosystem models, such as the APES model, are commonly validated against EC data, thus the agreement between the two methods is not surprising. However, as such models are driven by the continuous meteorological data and based on conservation of mass and energy, they provide strict physical constrains and may therefore be able to pinpoint problematic sections in EC data. In this study we found that such a multi-layer process-mechanistic model, which describes fluxes from leaf- to ecosystem-scale, was useful in bridging the gap between the other two methods, i.e. EC-based ecosystem scale GPP and Iso/SF giving species specific information on GPP.

The Iso/SF method has been constrained twice to deliver the seasonal pattern. First, periods with low VPD were filtered out, which occurred mostly at low temperatures, in order to exclude unreasonable stomatal conductance estimates. This is standard practice in the gas-exchange literature, (e.g., Stangl et al., 2019; Tarvainen et al., 2016). Second, the Iso/SF method weights the GPP estimates outside the growing season according to a temperature-driven model of photosynthetic capacity (Mäkelä et al., 2004). This double constraint had little effect for flux estimates in the middle of the growing season, but it

reduced variation in the spring and fall, forcing the method to produce the typical seasonal pattern.

The absolute values of GPP differed among methods, especially during the middle of the thermal growing season, in the order: $GPP_{A-PES} > GPP_{EC} > GPP_{Iso/SF}$ (Fig. 6). This can partly be attributed to the fact that EC estimate depends on the wind direction and speed and therefore may vary daily according to plot and species distribution. For example, if wind comes from the south, the fraction of PS would be higher (Fig. 1) than for the northern plots. In this example, the EC method would detect mostly GPP by PS and would lead to discrepancy in the entire footprint GPP, whereas APES always considers all plots/trees. Another explanation is to recognize that EC and APES estimate GPP at stand level whereas Iso/SF only estimates GPP for the two main overstory tree species. However, even after removing the understory contribution to the EC and APES estimates, we still observed the same ranking among the methods. Birch data are missing in the Iso/SF estimate, but the APES model results suggested that the contribution of birch to stand GPP was small (3.6 % of the overstory GPP).

Another possible explanation for the GPP mismatch is difficulties in the estimation of sap flux. This would translate into difficulties in the estimation of stomatal conductance, which is central to the Iso/SF method. The sap-flux technique is prone to several sources of error due to radial variability of sap flux in the trunk (Cohen et al., 2008; Ford et al., 2004; Renninger and Schäfer, 2012), azimuthal variability (Cohen et al., 2008), and calibration of the probe (Steppe et al., 2010; Sun et al., 2012). Several corrections have been proposed to account for these uncertainties (Clearwater et al., 1999; Peters et al., 2018; Steppe et al., 2010; Sun et al., 2012). Although we applied several of these corrections, there is reason to maintain some scepticism about their quantitative precision. This is particularly true because the data for pine agree so well, but the spruce GPP estimates are much lower than for the other methods. We discuss species differences in these traits below. Finally, Iso/SF method may be prone to a related upscaling uncertainties as the number of sampled trees is limited and may not represent exactly the stand features such as specific basal area or tree abundance per nodes. Likewise, WUE_i was just a mean of 10 trees per node. The 10 trees covered the diameter gradient of the stand, but it was not weighted according to the relative abundance of each specific size class.

By focusing on the summer months, when GPP is the highest, the difference among methods was also the highest (711, 582 and 431 gC m^{-2} for the GPP summer sum from APES, EC and Iso/SF respectively). This critical period deserves attention as it strongly affected the annual sum of GPP. It was out of the scope of this study to demonstrate that one approach is the truth, but our multi-method approach shows that this is also the period when D_Z and PPFD were the most variable.

A recent study showed that Iso/SF method was very sensitive to D_Z (Vernay et al., 2020). Similarly, the APES model may be prone to substantial error if the tree canopy structure is not accurate, which determines GPP according to the PPFD distribution in the canopy. As noted earlier, eddy covariance can be influenced by decoupling events, especially at night. A detailed comparison of eddy covariance to component fluxes at a nearby site failed to describe the changes induced by nitrogen fertilization (Marshall et al., 2023). It was not clear why the EC measurements failed to detect strong increases in soil organic matter and biomass accumulation (Marshall et al., 2023). To improve daily estimates of stand GPP, we suggest focusing on tree responses to D_Z (or VPD) and PPFD.

4.3. Difference in functional traits between species

The APES and Iso/SF methods can partition the GPP among the different tree species. In our study, we found a strong similarity for Scots pine GPP between APES and Iso/SF. but a large difference in Norway Spruce. The spruce discrepancy was highest during the summer and reduced in the fall. We speculate that the spruce sap flux measurements may have improved as temperatures fell, but focused work on this question is called for.

As mentioned in Section 2.2, LAI for spruce was higher than for pine but the modeled transpiration per leaf area was higher for pine. One explanation for the differences in spruce estimates could come to an overestimation of the light penetration in the canopy by the APES method. For instance, spruces were less abundant than pines but had a higher GPP contribution despite a lower photosynthetic capacity. Pines have a large part of their canopy exposed to light whereas spruce have a large part of their canopy at low light. Therefore, overestimating light access for spruce might contribute to a discrepancy to the advantage of their contribution. The APES discrepancy of understory GPP contribution compared to EC estimates also supports this hypothesis. A second, more probable hypothesis is that the difference for Norway Spruce between the two methods was due to the transpiration rate, which differed by 60 % between Iso/SF and APES. Transpiration is converted into canopy conductance, which is converted into GPP in the Iso/SF method. The most plausible explanation is the highly empirical methods to estimate zero flow in thermal dissipation methods, and how this affects the integration of the sap-flow radial profile. Under certain conditions, the outermost measurements (closest to the bark) of the conductive tissue reach zero flow at night, but the innermost area does not, and this pattern can be the exact opposite in some species. By forcing all nighttime values (or all values that meet the criteria of the method e.g., flatline for at least two hours, under low VPD) inside the sapwood depth to be zero, we are unintentionally influencing the radial profile shape, and thus the daily tree transpiration. The errors associated with the omission of radial profiles have been reported as greater than 150 % (Ford et al., 2004).

Moreover, the Iso/SF method filtered the g_S data outside the thermal growing season by correcting the value with a photosynthetic acclimation function. We used the same function for the two species but we acknowledge that it was first designed for Scots pine (Mäkelä et al., 2008, 2004). Recent studies showed that the parameterization of this function worked well for different species in different biomes, which made us confident about using it (Tian et al., 2020). However, other studies have demonstrated photosynthetic phenological differences between Scot pine and Norway spruce; Norway spruces have a longer active photosynthetic period, starting earlier and ending later than Scots pines (Linkosalo et al., 2014). Moreover, a recent study demonstrated a stronger photosynthetic recovery capacity for pines (Yang et al., 2020) that could influence the GPP, especially in early spring. The method might be improved by further attention to these species differences in seasonality.

Another explanation for the GPP differences between these species could be the choice of a constant g_S/g_m ratio in Eq. (6). Parameterizing g_m with this ratio allowed it to vary during the season according to g_S and thereby environmental conditions (Bickford et al., 2010; Montpied et al., 2009; Schiestl-Aalto et al., 2021; Stangl et al., 2019). Moreover, WUE_i is more strongly linked to g_S/g_m than to g_m itself, which should lead to a more reliable GPP estimate in our study (Nadal and Flexas, 2018). However, the ratio would not in fact be constant over the season (Stangl et al., 2022; Xiong et al., 2018). We assumed that the improvement of the $GPP_{Iso/SF}$ values would be negligible at the annual scale as the potential error would compensate between spring and fall.

Our isotopic measurements found a significant difference in WUE_i between the two species. Scots pines had a higher WUE_i than Norway spruces throughout the season. WUE_i is a simplification of WUE (Flexas et al., 2016; Sinclair et al., 1984) that neglects the dependence of WUE on VPD (Medlyn et al., 2017; Seibt et al., 2008). The Scots pine values were similar to the ones measured with the Iso/SF method in a nearby monospecific Scots pine forest (Vernay et al., 2020) and previous comparisons of pines and spruce (Marshall and Zhang, 1994). However, other studies have found higher WUE_i for Norway spruce compared to Scots pine, (e.g., Saurer et al., 2004). If WUE_i for Norway spruce were somehow underestimated, this could also partly explain the differences between Iso/SF and other GPP estimates. However, the spruce canopies

extended deeper into the canopy, where light intensities were lower. WUE_i is known to be reduced by shading in many conifer species (Duursma and Marshall, 2006). The lower values we observed in spruce may have been caused by these differences in vertical crown disposition, which might also be a reliable hypothesis to explain the WUE_i difference.

4.4. Understory vs overstory contribution

The EC and APES approaches were able to disaggregate overstory vs. understory GPP. The seasonal trend of understory GPP was consistent with the overstory's trend; EC estimated lower contributions than APES. The estimates were 6 and 11 % of the annual sum, i.e. 57 g C m^{-2} yr^{-1} and 97 g C m^{-2} yr^{-1} for EC and APES, respectively. These estimates were consistent with the low end of previous studies in Scots pine forests (Chi et al., 2021; Kulmala et al., 2011; Marshall et al., 2023; Tian et al., 2021) and a mixed Scots pine-Norway spruce forest (Palmroth et al., 2019). From an ecosystem partitioning perspective, the understory estimates suggest that they must be included in a complete boreal forest carbon budget.

4.5. Uncertainty budget

This exercise highlights the potential value of ecosystem uncertainty budgets for each of the methods. Such budgets would identify the uncertainties at each step of the inferences based on a mixture of theoretical or statistical methods of error propagation (Csavina et al., 2017; Harmon et al., 2015; Yanai et al., 2021). It would, for example, quantify uncertainties from the regression lines fit to calibration curves and from the standard deviations of summed fluxes (e.g., Roberti et al., 2014). Although such analysis is beyond the scope of the current study, we recognize its potential value and hope to see it in the future.

5. Conclusion

GPP is a key variable in the C balance of a forest but there are several ways to estimate it, which rely on different assumptions. In this study, the comparison between three approaches, eddy covariance, a biophysical model (APES), and an ecophysiological method (Iso/SF) showed that all approaches provide the same global seasonal pattern of GPP. All can be used for estimating GPP at stand scale. The most prominent and compelling matches were: first, the similarity in estimates of overstory GPP of pine by APES and Iso/SF. This is encouraging because the two methods are nearly independent. The second prominent match was between GPP_{EC} and GPP_{APES}, which however was expected based on earlier studies. The multi-method/models approach adds value as it narrows the search for discrepancies to certain strata and/or species; it also highlights the roles of different functional traits because of their sensitivity to different environmental factors. Indeed, the study allowed us to determine when the methods match and to speculate as to why the methods might mismatch. The clearest mismatch was between the descriptions of GPP by Iso/SF and APES in spruce, and the resulting discrepancy of total overstory GPP by Iso/SF compared to the other approaches. We speculate that there may be problems with the inference of stomatal conductance from sap flux in spruce. We looked for a second mismatch due to the inability of $GPP_{Iso/SF}$ to account for understory GPP, however it appeared negligible based on understory estimates by both GPP_{EC} and GPP_{APES}. Finally, PPFD and especially VPD were key variables in many of the calculations, especially when they were near zero, as during much of the spring and fall. Their influence on each of the methods deserves careful scrutiny. In our opinion, all methods provide complementary information: when EC flux provides an ecosystem overview of gas exchanges, APES and Iso/SF should be able to determine the contribution of each species to global GPP. The apparent discrepancy of GPP by spruce in the Iso/SF estimates suggests that there may be problems in the absolute values of the spruce sap-flux data. This kind of comparison might thus serve as a test of the sap-flux data at other sites.

Author's contributions

J.D.M and N.H designed the experiment. All authors conceived the ideas of the method comparison. K.L run the APES method. J.C and A.K performed the EC analysis. J.G.L. made the sap flow measurements and provided transpiration data, Z.R.S and A.V collected phloem samples and performed the Iso/SF with J.D.M. AV wrote the first version of the manuscript. All authors contributed to the different drafts of the manuscript and gave final approval for publication.

CRediT authorship contribution statement

Antoine Vernay: Data curation, Formal analysis, Validation, Writing – original draft, Writing – review & editing. **Niles Hasselquist:** Conceptualization, Data curation, Funding acquisition, Supervision. **Kersti Leppä:** Data curation, Formal analysis, Writing – review & editing. **Anne Klosterhalfen:** Data curation, Formal analysis, Writing – review & editing. **Jose Gutierrez Lopez:** Data curation, Formal analysis, Writing – review & editing. **Zsofia R Stangl:** Data curation, Formal analysis, Writing – review & editing. **Jinshu Chi:** Data curation, Formal analysis, Writing – review & editing. **Nathaliia Kozii:** Data curation, Writing – review & editing. **John D Marshall:** Conceptualization, Data curation, Formal analysis, Funding acquisition, Project administration, Supervision, Validation, Writing – review & editing.

Declaration of Competing Interest

The authors declare that they have no known competing financial interests or personal relationships that could have appeared to influence the work reported in this paper.

Data availability

Data will be made available on request.

Acknowledgement

Appendix

Fig. A1. Seasonal transpiration and evapotranspiration comparison between the Iso/SF, APES and EC. Grey area represents the thermal growing season. Loess trend lines and 95 % confidence intervals were added.

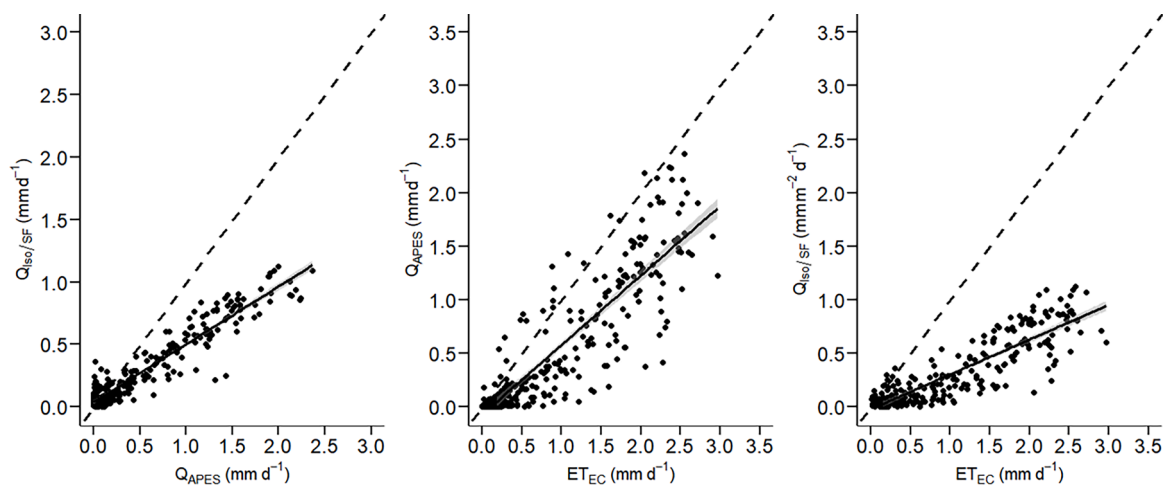**Fig. A2.** Paired annual transpiration (Q) and evapotranspiration (ET) comparison between the Iso/SF, APES and EC methods. Deming trend lines and 95 % confidence intervals were added.
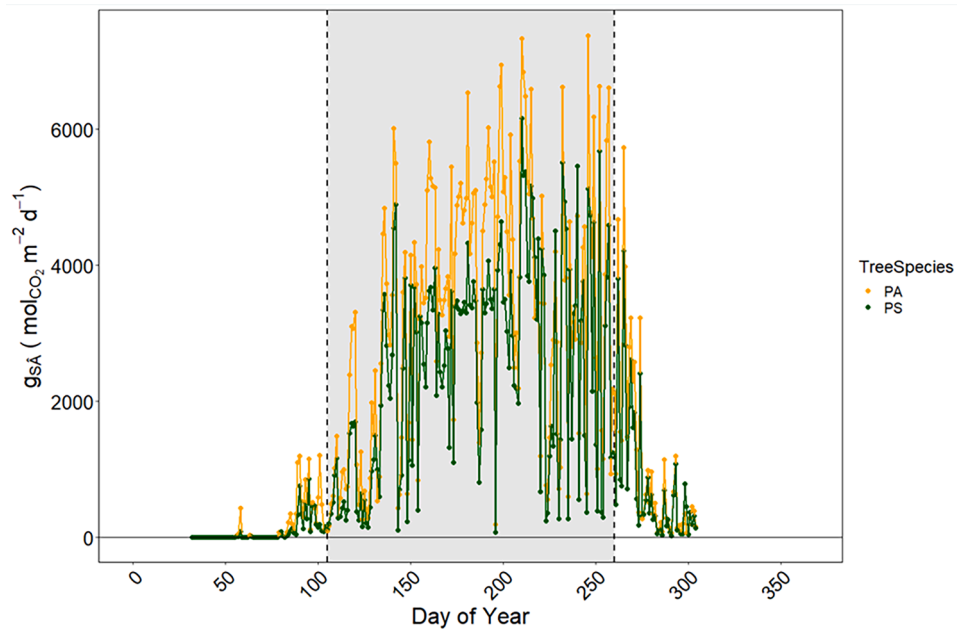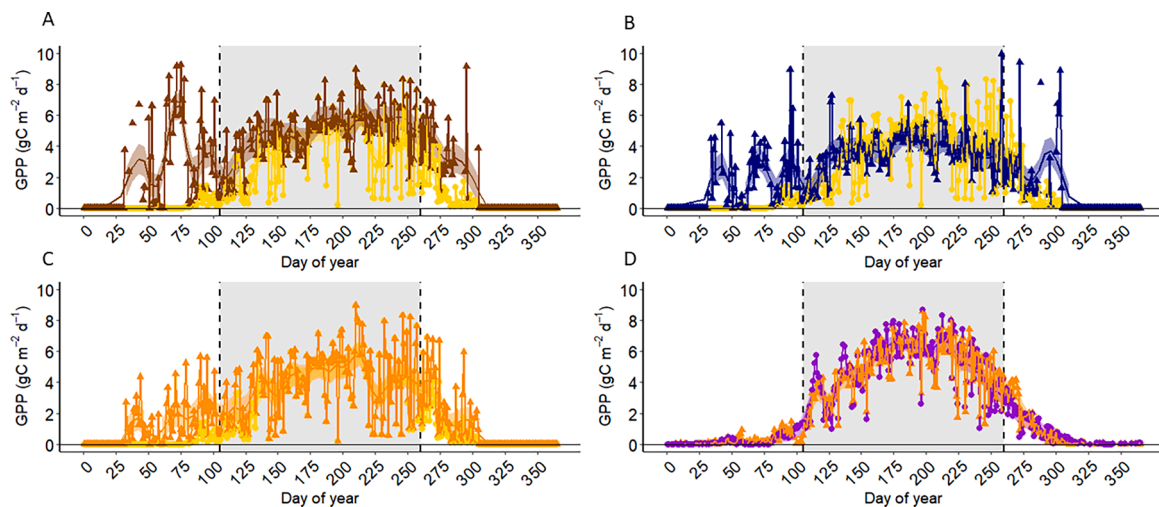

Fig. A3. Stomatal conductance corrected by Â ($g_{SÂ}$, mol_{CO2} m^{-2} d^{-1}) for Norway spruce (PA, yellow) and Scots pine (PS, green) in Iso/SF method. Grey area represents the thermal growing season.

Fig. A4. Seasonal GPP comparison between the Iso/SF method chosen for multi-method comparison in the article (gold line in graphs A,B and C) with the same method but without considering some applied filters. The graph A compares the GPP from Iso/SF method with the from Iso/SF method without considering Dz (brown line), or daytime VPD (blue line, B), or Â correction (orange line, C). The last graph (D) shows the EC estimates with considering nighttime or not. Grey area represents the thermal growing season.
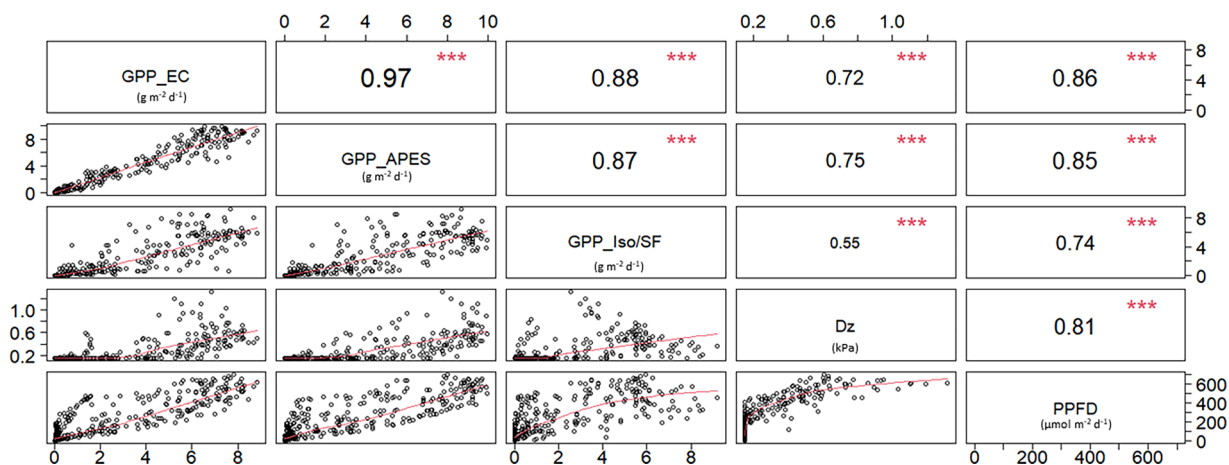
Fig. A5. Pairwise Spearman correlations between GPP estimates during the thermal growing season (eddy covariance (GPP_EC), APES (GPP_APES) and Iso/SF (GPP_Iso/SF) estimates respectively), daily normalized vapour pressure deficit (Dz, kPa), and photosynthetic active photonflux density (PPFD, µmol $m^{-2} s^{-1}$). Plots show the crossed-comparison between each variable. Numbers in the panels are the Spearman coefficient of correlation. *, **, *** correspond to $p < 0.1, 0.05, 0.01$ and 0.001, respectively.

References

Baldocchi, D.D., 2020. How eddy covariance flux measurements have contributed to our understanding of Global Change Biology. Global Change Biol. 26, 242–260.

Baldocchi, D.D., 2014. Measuring fluxes of trace gases and energy between ecosystems and the atmosphere – the state and future of the eddy covariance method. Global Change Biol. 20, 3600–3609. https://doi.org/10.1111/gcb.12649.

Baldocchi, D.D., 2003. Assessing the eddy covariance technique for evaluating carbon dioxide exchange rates of ecosystems: past, present and future. Global Change Biol. 9, 479–492. https://doi.org/10.1046/j.1365-2486.2003.00629.x.

Baldocchi, D.D., Wilson, K.B., Gu, L., 2002. How the environment, canopy structure and canopy physiological functioning influence carbon, water and energy fluxes of a temperate broad-leaved deciduous forest—An assessment with the biophysical model CANOAK. Tree Physiol. 22, 1065–1077. https://doi.org/10.1093/treephys/22.15-16.1065.

Berdanier, A.B., Miniat, C.F., Clark, J.S., 2016. Predictive models for radial sap flux variation in coniferous, diffuse-porous and ring-porous temperate trees. Tree Physiol. 36, 932–941. https://doi.org/10.1093/treephys/tpw027.

Bickford, C.P., Hanson, D.T., McDowell, N.G., 2010. Influence of diurnal variation in mesophyll conductance on modelled 13C discrimination: results from a field study. J. Exp. Bot. 61, 3223–3233. https://doi.org/10.1093/jxb/erq137.

Burba, G., 2019. Illustrative maps of past and present eddy covariance measurement locations: I. Early update.

Busch, F.A., Holloway-Phillips, M., Stuart-Williams, H., Farquhar, G.D., 2020. Revisiting carbon isotope discrimination in C 3 plants shows respiration rules when

photosynthesis is low. Nat. Plants 6, 245–258. https://doi.org/10.1038/s41477-020-0606-6.

Campioli, M., Malhi, Y., Vicca, S., Luyssaert, S., Papale, D., Peñuelas, J., Reichstein, M., Migliavacca, M., Arain, M.A., Janssens, I.A., 2016. Evaluating the convergence between eddy-covariance and biometric methods for assessing carbon budgets of forests. Nat. Commun. 7, 13717. https://doi.org/10.1038/ncomms13717.

Caylor, K.K., Dragoni, D., 2009. Decoupling structural and environmental determinants of sap velocity: Part I. Methodological development. Agricultural and Forest Meteorology 149, 559–569. https://doi.org/10.1016/j.agrformet.2008.10.006.

Charrier, G., Nolf, M., Leitinger, G., Charra-Vaskou, K., Losso, A., Tappeiner, U., Améglio, T., Mayr, S., 2017. Monitoring of Freezing Dynamics in Trees: A Simple Phase Shift Causes Complexity. Plant Physiol. 173, 2196–2207. https://doi.org/10.1104/pp.16.01815.

Chi, J., Nilsson, M.B., Kljun, N., Wallerman, J., Fransson, J.E.S., Laudon, H., Lundmark, T., Peichl, M., 2019. The carbon balance of a managed boreal landscape measured from a tall tower in northern Sweden. Agric. For. Meteorol. 274, 29–41. https://doi.org/10.1016/j.agrformet.2019.04.010.

Chi, J., Zhao, P., Klosterhalfen, A., Jocher, G., Kljun, N., Nilsson, M.B., Peichl, M., 2021. Forest floor fluxes drive differences in the carbon balance of contrasting boreal forest stands. Agric. For. Meteorol. 306, 108454 https://doi.org/10.1016/j.agrformet.2021.108454.

Clearwater, M.J., Meinzer, F.C., Andrade, J.L., Goldstein, G., Holbrook, N.M., 1999. Potential errors in measurement of nonuniform sap flow using heat dissipation probes. Tree Physiol. 19, 681–687. https://doi.org/10.1093/treephys/19.10.681.

Cleveland, W., Grosse, E., Shyu, W., 1992. Local regression models. Chapter 8 in Statistical models in S (JM Chambers and TJ Hastie eds.). Wadsworth & Brooks/Cole, Pacific Grove, CA, 608 p.

Cohen, Y., Cohen, S., Cantuarias-Aviles, T., Schiller, G., 2008. Variations in the radial gradient of sap velocity in trunks of forest and fruit trees. Plant Soil 305, 49–59. https://doi.org/10.1007/s11104-007-9351-0.

Cornes, R.C., Schrier, G.van der, Squintu, A.A., 2019. A reappraisal of the thermal growing season length across Europe. Int. J. Climatol. 39, 1787–1795. https://doi.org/10.1002/joc.5913.

Csavina, J., Roberti, J.A., Taylor, J.R., Loescher, H.W., 2017. Traceable measurements and calibration: a primer on uncertainty analysis. Ecosphere 8, e01683. https://doi.org/10.1002/ecs2.1683.

Duursma, R.A., Marshall, J.D., 2006. Vertical canopy gradients in δ13C correspond with leaf nitrogen content in a mixed-species conifer forest. Trees 20, 496–506.

Evans, J.R., Caemmerer, S.V., 2013. Temperature response of carbon isotope discrimination and mesophyll conductance in tobacco. Plant, Cell Environ. 36, 745–756. https://doi.org/10.1111/j.1365-3040.2012.02591.x.

Falge, E., Aubinet, M., Bakwin, P.S., Baldocchi, D., Berbigier, P., Bernhofer, C., Black, T. A., Ceulemans, R., Davis, K.J., Dolman, A.J., Goldstein, A., Goulden, M.L., Granier, A., Hollinger, D.Y., Jarvis, P.G., Jensen, N., Pilegaard, K., Katul, G., Kyaw Tha Paw, P., Law, B.E., Lindroth, A., Loustau, D., Mahli, Y., Monson, R., Moncrieff, P., Moors, E., Munger, J.W., Meyers, T., Oechel, W., Schulze, E.D., Thorgeirssen, H., Tenhunen, J., Valentini, R., Verma, S.B., Vesala, T., Wofsy, S.C., 2017. FLUXNET Research network site characteristics, investigators, and bibliography, 2016. https://doi.org/10.3334/ORNLDAAC/1530.

Farquhar, G.D., von Caemmerer, S., Berry, J.A., 1980. A biochemical model of photosynthetic CO2 assimilation in leaves of C3 species. Planta 149, 78–90. https://doi.org/10.1007/BF00386231.

Flexas, J., Díaz-Espejo, A., Conesa, M.A., Coopman, R.E., Douthe, C., Gago, J., Gallé, A., Galmés, J., Medrano, H., Ribas-Carbo, M., Tomàs, M., Niinemets, Ü., 2016. Mesophyll conductance to CO2 and Rubisco as targets for improving intrinsic water use efficiency in C3 plants. Plant, Cell Environ. 39, 965–982. https://doi.org/10.1111/pce.12622.

Flo, V., Martinez-Vilalta, J., Steppe, K., Schuldt, B., Poyatos, R., 2019. A synthesis of bias and uncertainty in sap flow methods. Agric. For. Meteorol. 271, 362–374. https://doi.org/10.1016/j.agrformet.2019.03.012.

Ford, C.R., McGuire, M.A., Mitchell, R.J., Teskey, R.O., 2004. Assessing variation in the radial profile of sap flux density in Pinus species and its effect on daily water use. Tree Physiol. 24, 241–249. https://doi.org/10.1093/treephys/24.3.241.

Gerle, F., Malherbe, P., Boisselet, C., Lafleuriel, D., Godfroy, J., Lochin, P., Marteau, B., Piegay, P., Puijalon, S., Vernay, A. Intrinsic water use efficiency estimate: an isotopic method. 2023.doi: 10.17504/protocols.io.dm6gp3xk8vzp/v1.

Gessler, A., Rennenberg, H., Keitel, C., 2004. Stable isotope composition of organic compounds transported in the phloem of european beech - Evaluation of different methods of phloem sap collection and assessment of gradients in carbon isotope composition during leaf-to-stem transport. Plant Biol. 6, 721–729. https://doi.org/10.1055/s-2004-830350.

Granier, A., 1987. Evaluation of transpiration in a Douglas-fir stand by means of sap flow measurements. Tree Physiol. 3, 309–320. https://doi.org/10.1093/treephys/3.4.309.

Granier, A., 1985. Une nouvelle méthode pour la mesure du flux de sève brute dans le tronc des arbres. Ann. Sci. For. 42, 193–200.

Granier, A., Anfodillo, T., Sabatti, M., Cochard, H., Dreyer, E., Tomasi, M., Valentini, R., Bréda, N., 1994. Axial and radial water flow in the trunks of oak trees: a quantitative and qualitative analysis. Tree Physiol. 14, 1383–1396.

Grime, J.P., 1998. Benefits of plant diversity to ecosystems: immediate, filter and founder effects. J. Ecol. 86, 902–910. https://doi.org/10.1046/j.1365-2745.1998.00306.x.

Gutiérrez López, J., 2015. Construction of Heat Dissipation Probes to Estimate Sap Flow. Ecohydrology Laboratory-University of New Hampshire, Durham, NH, USA.

Gutierrez Lopez, J., Tor-ngern, P., Oren, R., Kozii, N., Laudon, H., Hasselquist, N.J., 2021. How tree species, tree size, and topographical location influenced tree transpiration in northern boreal forests during the historic 2018 drought. Global Change Biol. 27, 3066–3078. https://doi.org/10.1111/gcb.15601.

Härkönen, S., Lehtonen, A., Manninen, T., Tuominen, S., Peltoniemi, M., 2015. Estimating forest leaf area index using satellite images: comparison of k-NN based Landsat-NFI LAI with MODIS-RSR based LAI product for Finland.

Harmon, M.E., Fasth, B., Halpern, C.B., Lutz, J.A., 2015. Uncertainty analysis: an evaluation metric for synthesis science. Ecosphere 6, art63. https://doi.org/10.1890/ES14-00235.1.

Hollinger, D.Y., Richardson, A.D., 2005. Uncertainty in eddy covariance measurements and its application to physiological models. Tree Physiol. 25, 873–885. https://doi.org/10.1093/treephys/25.7.873.

Hu, J., Moore, D.J.P., Riveros-Iregui, D.A., Burns, S.P., Monson, R.K., 2010. Modeling whole-tree carbon assimilation rate using observed transpiration rates and needle sugar carbon isotope ratios. New Phytol. 185, 1000–1015. https://doi.org/10.1111/j.1469-8137.2009.03154.x.

Ikawa, H., Nakai, T., Busey, R.C., Kim, Y., Kobayashi, H., Nagai, S., Ueyama, M., Saito, K., Nagano, H., Suzuki, R., Hinzman, L., 2015. Understory CO2, sensible heat, and latent heat fluxes in a black spruce forest in interior Alaska. Agric. For. Meteorol. 214–215, 80–90. https://doi.org/10.1016/j.agrformet.2015.08.247.

Jocher, G., Ottosson Löfvenius, M., De Simon, G., Hörnlund, T., Linder, S., Lundmark, T., Marshall, J., Nilsson, M.B., Näsholm, T., Tarvainen, L., Öquist, M., Peichl, M., 2017. Apparent winter CO2 uptake by a boreal forest due to decoupling. Agric. For. Meteorol. 232, 23–34. https://doi.org/10.1016/j.agrformet.2016.08.002.

Jung, M., Schwalm, C., Migliavacca, M., Walther, S., Camps-Valls, G., Koirala, S., Anthoni, P., Besnard, S., Bodesheim, P., Carvalhais, N., Chevallier, F., Gans, F., Goll, D.S., Haverd, V., Köhler, P., Ichii, K., Jain, A.K., Liu, J., Lombardozzi, D., Nabel, J.E.M.S., Nelson, J.A., O'Sullivan, M., Pallandt, M., Papale, D., Peters, W., Pongratz, J., Rödenbeck, C., Sitch, S., Tramontana, G., Walker, A., Weber, U.,

Reichstein, M., 2020. Scaling carbon fluxes from eddy covariance sites to globe: synthesis and evaluation of the FLUXCOM approach. Biogeosciences 17, 1343–1365. https://doi.org/10.5194/bg-17-1343-2020.

Kim, H.S., Oren, R., Hinckley, T.M., 2008. Actual and potential transpiration and carbon assimilation in an irrigated poplar plantation. Tree Physiol. 28, 559–577. https://doi.org/10.1093/treephys/28.4.559.

Kitin, P., Voelker, S.L., Meinzer, F.C., Beeckman, H., Strauss, S.H., Lachenbruch, B., 2010. Tyloses and Phenolic Deposits in Xylem Vessels Impede Water Transport in Low-Lignin Transgenic Poplars: A Study by Cryo-Fluorescence Microscopy. Plant Physiol. 154, 887–898. https://doi.org/10.1104/pp.110.156224.

Klein, T., Rotenberg, E., Tatarinov, F., Yakir, D., 2016. Association between sap flow-derived and eddy covariance-derived measurements of forest canopy CO2 uptake. New Phytol. 209, 436–446. https://doi.org/10.1111/nph.13597.

Kljun, N., Calanca, P., Rotach, M., Schmid, H.P., 2015. A simple two-dimensional parameterisation for Flux Footprint Prediction (FFP). Geosci. Model. Dev. 8, 3695.

Klosterhalfen, A., Graf, A., Brüggemann, N., Drüe, C., Esser, O., González-Dugo, M.P., Heinemann, G., Jacobs, C.M., Mauder, M., Moene, A.F., 2019. Source partitioning of H2 O and CO2 fluxes based on high-frequency eddy covariance data: a comparison between study sites. Biogeosciences 16, 1111–1132.

Kooijmans, L.M.J., Maseyk, K., Seibt, U., Sun, W., Vesala, T., Mammarella, I., Kolari, P., Aalto, J., Franchin, A., Vecchi, R., Valli, G., Chen, H., 2017. Canopy uptake dominates nighttime carbonyl sulfide fluxes in a boreal forest. Atmos. Chem. Phys. 17, 11453–11465. https://doi.org/10.5194/acp-17-11453-2017.

Kottek, M., Grieser, J., Beck, C., Rudolf, B., Rubel, F., 2006. World map of the Köppen-Geiger climate classification updated. Meteorol. Z. 15, 259–263. https://doi.org/10.1127/0941-2948/2006/0130.

Kozii, N., Haahti, K., Tor-ngern, P., Chi, J., Hasselquist, E.M., Laudon, H., Launiainen, S., Oren, R., Peichl, M., Wallerman, J., 2019. Partitioning the forest water balance within a boreal catchment using sapflux, eddy covariance and process-based model. Hydrol. Earth Syst. Sci. Discuss. 1–50.

Kulmala, L., Pumpanen, J., Kolari, P., Muukkonen, P., Hari, P., Vesala, T., 2011. Photosynthetic production of ground vegetation in different-aged Scots pine (Pinus sylvestris) forests. Can. J. For. Res. 41, 2020–2030. https://doi.org/10.1139/x11-121.

Lasslop, G., Reichstein, M., Papale, D., Richardson, A.D., Arneth, A., Barr, A., Stoy, P., Wohlfahrt, G., 2010. Separation of net ecosystem exchange into assimilation and respiration using a light response curve approach: critical issues and global evaluation. Global Change Biol. 16, 187–208. https://doi.org/10.1111/j.1365-2486.2009.02041.x.

Laudon, H., Hasselquist, E.M., Peichl, M., Lindgren, K., Sponseller, R., Lidman, F., Kuglerová, L., Hasselquist, N.J., Bishop, K., Nilsson, M.B., Ågren, A.M., 2021. Northern landscapes in transition: Evidence, approach and ways forward using the Krycklan Catchment Study. Hydrol. Processes 35, e14170. https://doi.org/10.1002/hyp.14170.

Laudon, H., Taberman, I., Ågren, A., Futter, M., Ottosson-Löfvenius, M., Bishop, K., 2013. The Krycklan catchment study—A flagship infrastructure for hydrology, biogeochemistry, and climate research in the boreal landscape. Water Resour. Res. 49, 7154–7158. https://doi.org/10.1002/wrcr.20520.

Launiainen, S., Guan, M., Salmivaara, A., Kieloaho, A.J., 2019. Modeling boreal forest evapotranspiration and water balance at stand and catchment scales: a spatial approach. Hydrol. Earth Syst. Sci. 23, 3457–3480.

Launiainen, S., Katul, G.G., Lauren, A., Kolari, P., 2015. Coupling boreal forest CO2, H2O and energy flows by a vertically structured forest canopy – Soil model with separate bryophyte layer. Ecol. Modell. 312, 385–405. https://doi.org/10.1016/j.ecolmodel.2015.06.007.

Ledesma, J.L.J., Futter, M.N., Laudon, H., Evans, C.D., Köhler, S.J., 2016. Boreal forest riparian zones regulate stream sulfate and dissolved organic carbon. Sci. Total Environ. 560–561, 110–122. https://doi.org/10.1016/j.scitotenv.2016.03.230.

Lehtonen, A., Heikkinen, J., Petersson, H., Ťupek, B., Liski, E., Mäkelä, A., 2019. Scots pine and Norway spruce foliage biomass in Finland and Sweden — Testing traditional models vs. the pipe model theory. Can. J. For. Res. https://doi.org/10.1139/cjfr-2019-0211.

Linkosalo, T., Heikkinen, J., Pulkkinen, P., Mäkipää, R., 2014. Fluorescence measurements show stronger cold inhibition of photosynthetic light reactions in Scots pine compared to Norway spruce as well as during spring compared to autumn. Front. Plant. Sci. 5, 264. https://doi.org/10.3389/fpls.2014.00264.

Loescher, H.W., Law, B.E., Mahrt, L., Hollinger, D.Y., Campbell, J., Wofsy, S.C., 2006. Uncertainties in, and interpretation of, carbon flux estimates using the eddy covariance technique. J. Geophys. Res. Atmos. 111 https://doi.org/10.1029/2005JD006932.

Luyssaert, S., Inglima, I., Jung, M., Richardson, A.D., Reichstein, M., Papale, D., Piao, S. L., Schulze, E.D., Wingate, L., Matteucci, G., Aragao, L., Aubinet, M., Beer, C., Bernhofer, C., Black, K.G., Bonal, D., Bonnefond, J.M., Chambers, J., Ciais, P., Cook, B., Davis, K.J., Dolman, A.J., Gielen, B., Goulden, M., Grace, J., Granier, A., Grelle, A., Griffis, T., Grünwald, T., Guidolotti, G., Hanson, P.J., Harding, R., Hollinger, D.Y., Hutyra, L.R., Kolari, P., Kruijt, B., Kutsch, W., Lagergren, F., Laurila, T., Law, B.E., Maire, G., Lindroth, A., Loustau, D., Malhi, Y., Mateus, J., Migliavacca, M., Misson, L., Montagnani, L., Moncrieff, J., Moors, E., Munger, J.W., Nikinmaa, E., Ollinger, S.V., Pita, G., Rebmann, C., Roupsard, O., Saigusa, N., Sanz, M.J., Seufert, G., Sierra, C., Smith, M.L., Tang, J., Valentini, R., Vesala, T., Janssens, I.A., 2007. CO2 balance of boreal, temperate, and tropical forests derived from a global database. Global Change Biol. 13, 2509–2537. https://doi.org/10.1111/j.1365-2486.2007.01439.x.

Mäkelä, A., Hari, P., Berninger, F., Hänninen, H., Nikinmaa, E., 2004. Acclimation of photosynthetic capacity in Scots pine to the annual cycle of temperature. Tree Physiol. 24, 369–376. https://doi.org/10.1093/treephys/24.4.369.

Mäkelä, A., Kolari, P., Karimäki, J., Nikinmaa, E., Perämäki, M., Hari, P., 2006. Modelling five years of weather-driven variation of GPP in a boreal forest. Agric. For. Meteorol. 139, 382–398. https://doi.org/10.1016/j.agrformet.2006.08.017.

Mäkelä, A., Pulkkinen, M., Kolari, P., Lagergren, F., Berbigier, P., Lindroth, A., Loustau, D., Nikinmaa, E., Vesala, T., Hari, P., 2008. Developing an empirical model of stand GPP with the LUE approach: analysis of eddy covariance data at five contrasting conifer sites in Europe. Glob. Change Biol. 14, 92–108. https://doi.org/10.1111/j.1365-2486.2007.01463.x.

Marshall, J.D., Tarvainen, L., Zhao, P., Lim, H., Wallin, G., Näsholm, T., Lundmark, T., Linder, S., Peichl, M., 2023. Components explain, but do eddy fluxes constrain? Carbon budget of a nitrogen-fertilized boreal Scots pine forest. New Phytol. https://doi.org/10.1111/nph.18939.

Marshall, J.D., Zhang, J., 1994. Carbon Isotope Discrimination and Water-Use Efficiency in Native Plants of the North-Central Rockies. Ecology 75, 1887–1895. https://doi.org/10.2307/1941593.

McElrone, A.J., Grant, J.A., Kluepfel, D.A., 2010. The role of tyloses in crown hydraulic failure of mature walnut trees afflicted by apoplexy disorder. Tree Physiol. 30, 761–772. https://doi.org/10.1093/treephys/tpq026.

Medlyn, B.E., Dreyer, E., Ellsworth, D., Forstreuter, M., Harley, P.C., Kirschbaum, M.U.F., Roux, X.L., Montpied, P., Strassemeyer, J., Walcroft, A., Wang, K., Loustau, D., 2002. Temperature response of parameters of a biochemically based model of photosynthesis. II. A review of experimental data. Plant, Cell Environ. 25, 1167–1179. https://doi.org/10.1046/j.1365-3040.2002.00891.x.

Medlyn, B.E., Duursma, R.A., Eamus, D., Ellsworth, D.S., Prentice, I.C., Barton, C.V.M., Crous, K.Y., Angelis, P.D., Freeman, M., Wingate, L., 2011. Reconciling the optimal and empirical approaches to modelling stomatal conductance. Global Change Biol. 17, 2134–2144. https://doi.org/10.1111/j.1365-2486.2010.02375.x.

Medlyn, B.E., Kauwe, M.G.D., Lin, Y.S., Knauer, J., Duursma, R.A., Williams, C.A., Arneth, A., Clement, R., Isaac, P., Limousin, J.M., Linderson, M.L., Meir, P., Martin-StPaul, N., Wingate, L., 2017. How do leaf and ecosystem measures of water-use efficiency compare? New Phytol. 216, 758–770. https://doi.org/10.1111/nph.14626.

Minunno, F., Peltoniemi, M., Launiainen, S., Aurela, M., Lindroth, A., Lohila, A., Mammarella, I., Minkkinen, K., Mäkelä, A., 2016. Calibration and validation of a semi-empirical flux ecosystem model for coniferous forests in the Boreal region. Ecol. Modell. 341, 37–52. https://doi.org/10.1016/j.ecolmodel.2016.09.020.

Misson, L., Baldocchi, D.D., Black, T.A., Blanken, P.D., Brunet, Y., Curiel Yuste, J., Dorsey, J.R., Falk, M., Granier, A., Irvine, M.R., Jarosz, N, Lamaud, E., Launiainen, S., Law, B.E., Longdoz, B., Loustau, D., McKay, M., Paw U, K.T., Vesala, T., Vickers, D., Wilson, K.B., Goldstein, A.H., 2007. Partitioning forest carbon fluxes with overstory and understory eddy-covariance measurements: A synthesis based on FLUXNET data. Agric. For. Meteorol. 144, 14–31. https://doi.org/10.1016/j.agrformet.2007.01.006.

Montagnani, L., Grünwald, T., Kowalski, A., Mammarella, I., Merbold, L., Metzger, S., Sedlák, P., Siebicke, L., 2018. Estimating the storage term in eddy covariance measurements: the ICOS methodology. Int. Agrophys. 32, 551–567. https://doi.org/10.3929/ethz-b-000313349.

Montpied, P., Granier, A., Dreyer, E., 2009. Seasonal time-course of gradients of photosynthetic capacity and mesophyll conductance to CO2 across a beech (Fagus sylvatica L.) canopy. J. Exp. Bot. 60, 2407–2418. https://doi.org/10.1093/jxb/erp093.

Nadal, M., Flexas, J., 2018. Mesophyll conductance to CO2 diffusion: Effects of drought and opportunities for improvement. In: García Tejero, I.F., Durán Zuazo, V.H. (Eds.), Water Scarcity and Sustainable Agriculture in Semiarid Environment. Academic Press, pp. 403–438. https://doi.org/10.1016/B978-0-12-813164-0.00017-X.

Ngao, J., Adam, B., Saudreau, M., 2017. Intra-crown spatial variability of leaf temperature and stomatal conductance enhanced by drought in apple tree as assessed by the RATP model. Agric. For. Meteorol. 237–238, 340–354. https://doi.org/10.1016/j.agrformet.2017.02.036.

Ogée, J., Brunet, Y., Loustau, D., Berbigier, P., Delzon, S., 2003. MuSICA, a CO2, water and energy multilayer, multileaf pine forest model: evaluation from hourly to yearly time scales and sensitivity analysis. Global Change Biol. 9, 697–717. https://doi.org/10.1046/j.1365-2486.2003.00628.x.

Oren, R., Phillips, N., Ewers, B.E., Pataki, D.E., Megonigal, J.P., 1999. Sap-flux-scaled transpiration responses to light, vapor pressure deficit, and leaf area reduction in a flooded Taxodium distichum forest. Tree Physiol. 19, 337–347. https://doi.org/10.1093/treephys/19.6.337.

Oren, R., Zimmermann, R., Terbough, J., 1996. Transpiration in upper amazonia floodplain and upland forests in response to drought-breaking rains. Ecology 77, 968–973. https://doi.org/10.2307/2265517.

Ouimette, A.P., Ollinger, S.V., Richardson, A.D., Hollinger, D.Y., Keenan, T.F., Lepine, L.C., Vadeboncoeur, M.A., 2018. Carbon fluxes and interannual drivers in a temperate forest ecosystem assessed through comparison of top-down and bottom-up approaches. Agric. For. Meteorol. 256–257, 420–430. https://doi.org/10.1016/j.agrformet.2018.03.017.

Palmroth, S., Bach, L.H., Lindh, M., Kolari, P., Nordin, A., Palmqvist, K., 2019. Nitrogen supply and other controls of carbon uptake of understory vegetation in a boreal Picea abies forest. Agric. For. Meteorol. 276–277, 107620 https://doi.org/10.1016/j.agrformet.2019.107620.

Peichl, M., Brodeur, J.J., Khomik, M., Arain, M.A., 2010. Biometric and eddy-covariance based estimates of carbon fluxes in an age-sequence of temperate pine forests. Agric. For. Meteorol. 150, 952–965. https://doi.org/10.1016/j.agrformet.2010.03.002.

Peters, R.L., Fonti, P., Frank, D.C., Poyatos, R., Pappas, C., Kahmen, A., Carraro, V., Prendin, A.L., Schneider, L., Baltzer, J.L., Baron-Gafford, G.A., Dietrich, L., Heinrich, I., Minor, R.L., Sonnentag, O., Matheny, A.M., Wightman, M.G., Steppe, K., 2018. Quantification of uncertainties in conifer sap flow measured with the thermal dissipation method. New Phytol. 219, 1283–1299. https://doi.org/10.1111/nph.15241.

Pinheiro, J., Bates, D., DebRoy, S., Sarkar, D., 2016. R Core Team (2016) nlme: linear and nonlinear mixed effects models. R Package Version 3.1-128. Available at ht tps. cran. r-projectorg/web/packages/nlme/index. html. Accessed July 7.

R Core Team, 2016. R: A Language and Environment for Statistical Computing.

Reichstein, M., Falge, E., Baldocchi, D., Papale, D., Aubinet, M., Berbigier, P., Bernhofer, C., Buchmann, N., Gilmanov, T., Granier, A., Grünwald, T., Havránková, K., Ilvesniemi, H., Janous, D., Knohl, A., Laurila, T., Lohila, A., Loustau, D., Matteucci, G., Meyers, T., Miglietta, F., Ourcival, J.M., Pumpanen, J., Rambal, S., Rotenberg, E., Sanz, M., Tenhunen, J., Seufert, G., Vaccari, F., Vesala, T., Yakir, D., Valentini, R., 2005. On the separation of net ecosystem exchange into assimilation and ecosystem respiration: review and improved algorithm. Global Change Biol. 11, 1424–1439. https://doi.org/10.1111/j.1365-2486.2005.001002.x.

Reichstein, M., Stoy, P.C., Desai, A.R., Lasslop, G., Richardson, A.D., 2012. Partitioning of net fluxes. Eddy Covariance. Springer, pp. 263–289.

Renninger, H.J., Schäfer, K.V.R., 2012. Comparison of tissue heat balance- and thermal dissipation-derived sap flow measurements in ring-porous oaks and a pine. Front. Plant. Sci. 3, 103. https://doi.org/10.3389/fpls.2012.00103.

Roberti, J.A., SanClements, M.D., Loescher, H.W., Ayres, E., 2014. Traceable Calibration, Performance Metrics, and Uncertainty Estimates of Minirhizotron Digital Imagery for Fine-Root Measurements. PLoS One 9, e112362. https://doi.org/10.1371/journal.pone.0112362.

Rstudio, T., 2020. RStudio: Integrated Development Environment for R.

Sabbatini, S., Mammarella, I., Arriga, N., Fratini, G., Graf, A., Hörtnagl, L., Ibrom, A., Longdoz, B., Mauder, M., Merbold, L., Metzger, S., Montagnani, L., Pitacco, A., Rebmann, C., Sedlák, P., Sigut, L., Vitale, D., Papale, D., 2018. Eddy covariance raw data processing for CO2 and energy fluxes calculation at ICOS ecosystem stations. Int. Agrophys. 32, 495–515. https://doi.org/10.3929/ethz-b-000313355.

Saurer, M., Siegwolf, R.T.W., Schweingruber, F.H., 2004. Carbon isotope discrimination indicates improving water-use efficiency of trees in northern Eurasia over the last 100 years. Global Change Biol. 10, 2109–2120. https://doi.org/10.1111/j.1365-2486.2004.00869.x.

Schäfer, K.V.R., Oren, R., Ellsworth, D.S., Lai, C.T., Herrick, J.D., Finzi, A.C., Richter, D.D., Katul, G.G., 2003. Exposure to an enriched CO2 atmosphere alters carbon assimilation and allocation in a pine forest ecosystem. Global Change Biol. 9, 1378–1400. https://doi.org/10.1046/j.1365-2486.2003.00662.x.

Schiestl-Aalto, P., Stangl, Z.R., Tarvainen, L., Wallin, G., Marshall, J., Mäkelä, A., 2021. Linking canopy-scale mesophyll conductance and phloem sugar δ13C using empirical and modelling approaches. New Phytol. 229, 3141–3155.

Seibt, U., Rajabi, A., Griffiths, H., Berry, J.A., 2008. Carbon isotopes and water use efficiency: sense and sensitivity. Oecologia 155, 441–454. https://doi.org/10.1007/s00442-007-0932-7.

Selin, L., 2020. Modeling of Effective Leaf Area Index.

Sinclair, T.R., Tanner, C.B., Bennett, J.M., 1984. Water-use efficiency in crop production. Bioscience 34, 36–40. https://doi.org/10.2307/1309424.

Stangl, Z.R., Tarvainen, L., Wallin, G., Marshall, J.D., 2022. Limits to photosynthesis: seasonal shifts in supply and demand for CO2 in Scots pine. New Phytol. 233, 1108–1120. https://doi.org/10.1111/nph.17856.

Stangl, Z.R., Tarvainen, L., Wallin, G., Ubierna, N., Räntfors, M., Marshall, J.D., 2019. Diurnal variation in mesophyll conductance and its influence on modelled water-use efficiency in a mature boreal Pinus sylvestris stand. Photosynth. Res. 141, 53–63. https://doi.org/10.1007/s11120-019-00645-6.

Steppe, K., De Pauw, D.J.W., Doody, T.M., Teskey, R.O., 2010. A comparison of sap flux density using thermal dissipation, heat pulse velocity and heat field deformation methods. Agric. For. Meteorol. 150, 1046–1056. https://doi.org/10.1016/j.agrformet.2010.04.004.

Stoy, P.C., Katul, G.G., Siqueira, M.B., Juang, J.Y., Novick, K.A., Uebelherr, J.M., Oren, R., 2006. An evaluation of models for partitioning eddy covariance-measured net ecosystem exchange into photosynthesis and respiration. Agric. For. Meteorol. 141, 2–18.

Sun, H., Aubrey, D.P., Teskey, R.O., 2012. A simple calibration improved the accuracy of the thermal dissipation technique for sap flow measurements in juvenile trees of six species. Trees 26, 631–640. https://doi.org/10.1007/s00468-011-0631-1.

Tahvanainen, T., Forss, E., 2008. Individual tree models for the crown biomass distribution of Scots pine, Norway spruce and birch in Finland. Forest Ecol. Manag. 255, 455–467. https://doi.org/10.1016/j.foreco.2007.09.035.

Tarvainen, Lasse, Martina, Lutz, Mats, Räntfors, Torgny, Näsholm, Göran, Wallin, 2016. Increased Needle Nitrogen Contents Did Not Improve Shoot Photosynthetic Performance of Mature Nitrogen-Poor Scots Pine Trees. Front. Plant Sci. 7, 1051-.

Thomas, C.K., Martin, J.G., Law, B.E., Davis, K., 2013. Toward biologically meaningful net carbon exchange estimates for tall, dense canopies: multi-level eddy covariance observations and canopy coupling regimes in a mature Douglas-fir forest in Oregon. Agric. For. Meteorol. 173, 14–27. https://doi.org/10.1016/j.agrformet.2013.01.001.

Tian, X., Minunno, F., Cao, T., Peltoniemi, M., Kalliokoski, T., Mäkelä, A., 2020. Extending the range of applicability of the semi-empirical ecosystem flux model PRELES for varying forest types and climate. Global Change Biol. 26, 2923–2943. https://doi.org/10.1111/gcb.14992.

Tian, X., Minunno, F., Schiestl-Aalto, P., Chi, J., Zhao, P., Peichl, M., Marshall, J., Näsholm, T., Lim, H., Peltoniemi, M., Linder, S., Mäkelä, A., 2021. Disaggregating the effects of nitrogen addition on gross primary production in a boreal Scots pine forest. Agric. For. Meteorol. 301–302, 108337 https://doi.org/10.1016/j.agrformet.2021.108337.

Tupek, B., Mäkipää, R., Heikkinen, J., Peltoniemi, M., Ukonmaanaho, L., Hokkanen, T., Nojd, P., Nevalainen, S., Lindgren, M., Lehtonen, A., 2015. Foliar turnover rates in

Finland-comparing estimates from needle-cohort and litterfall-biomass methods. Boreal Environ. Res.

Vernay, A., Tian, X., Chi, J., Linder, S., Mäkelä, A., Oren, R., Peichl, M., Stangl, Z.R., Tor-Ngern, P., Marshall, J.D., 2020. Estimating canopy gross primary production by combining phloem stable isotopes with canopy and mesophyll conductances. Plant, Cell Environ. 43, 2124–2142. https://doi.org/10.1111/pce.13835.

Wang, M., Guan, D.X., Han, S.J., Wu, J.L., 2010. Comparison of eddy covariance and chamber-based methods for measuring CO2 flux in a temperate mixed forest. Tree Physiol. 30, 149–163. https://doi.org/10.1093/treephys/tpp098.

Wang, X., Wang, C., Bond-Lamberty, B., 2017. Quantifying and reducing the differences in forest CO2-fluxes estimated by eddy covariance, biometric and chamber methods: A global synthesis. Agric. For. Meteorol. 247, 93–103. https://doi.org/10.1016/j.agrformet.2017.07.023.

Watanabe, T., Mizutani, K., 1996. Model study on micrometeorological aspects of rainfall interception over an evergreen broad-leaved forest. Agric. For. Meteorol. 80, 195–214. https://doi.org/10.1016/0168-1923(95)02301-1.

White, J.W.C., Vaughn, B.H., Michel, S.E., 2015. Stable isotopic composition of atmospheric carbon dioxide (13C and 18O) from the NOAA ESRL carbon cycle cooperative global air sampling network, 1990-2014, Version: 2015-10-26.

Wullschleger, S.D., King, A.W., 2000. Radial variation in sap velocity as a function of stem diameter and sapwood thickness in yellow-poplar trees. Tree Physiol. 20, 511–518.

Wutzler, T., Lucas-Moffat, A., Migliavacca, M., Knauer, J., Sickel, K., Šigut, L., Menzer, O., Reichstein, M., 2018. Basic and extensible post-processing of eddy covariance flux data with REddyProc. Biogeosciences 15, 5015–5030. https://doi.org/10.5194/bg-15-5015-2018.

Xiong, D., Douthe, C., Flexas, J., 2018. Differential coordination of stomatal conductance, mesophyll conductance, and leaf hydraulic conductance in response to changing light across species. Plant, Cell Environ. 41, 436–450. https://doi.org/10.1111/pce.13111.

Yanai, R.D., Mann, T.A., Hong, S.D., Pu, G., Zukswert, J.M., 2021. The current state of uncertainty reporting in ecosystem studies: a systematic evaluation of peer-reviewed literature. Ecosphere 12, e03535. https://doi.org/10.1002/ecs2.3535.

Yang, Q., Blanco, N.E., Hermida-Carrera, C., Lehotai, N., Hurry, V., Strand, Å., 2020. Two dominant boreal conifers use contrasting mechanisms to reactivate photosynthesis in the spring. Nat. Commun. 11, 128. https://doi.org/10.1038/s41467-019-13954-0.

Zhao, P., Lu, P., Ma, L., Sun, G., Rao, X., Cai, X., Zeng, X., 2005. Combining sap flow measurement-based canopy stomatal conductance and 13C discrimination to estimate forest carbon assimilation. Chin. Sci. Bull. 50, 2021–2027. https://doi.org/10.1007/BF03322795.

Zhao, W., Qualls, R.J., 2006. Modeling of long-wave and net radiation energy distribution within a homogeneous plant canopy via multiple scattering processes. Water Resour. Res. 42 https://doi.org/10.1029/2005WR004581.